

Analysis and Optimization of Caching and Multicasting in Large-Scale Cache-Enabled Wireless Networks

Ying Cui, *MIEEE*, Dongdong Jiang, *SMIEEE*, Yueping Wu, *MIEEE*

Abstract

Caching and multicasting at base stations are two promising approaches to support massive content delivery over wireless networks. However, existing analysis and designs do not fully explore and exploit the potential advantages of the two approaches. In this paper, we consider the analysis and optimization of caching and multicasting in a large-scale cache-enabled wireless network. We propose a random caching and multicasting scheme with a design parameter. By carefully handling different types of interferers and adopting appropriate approximations, we derive a tractable expression for the successful transmission probability in the general region, utilizing tools from stochastic geometry. We also obtain a closed-form expression for the successful transmission probability in the high signal-to-noise ratio (SNR) and user density region. Then, we consider the successful transmission probability maximization, which is a very complex non-convex problem in general. Using optimization techniques, we develop an iterative numerical algorithm to obtain a local optimal caching and multicasting design in the general region. To reduce complexity and maintain superior performance, we also derive an asymptotically optimal caching and multicasting design in the asymptotic region, based on a two-step optimization framework. Finally, numerical simulations show that the asymptotically optimal design achieves a significant gain in successful transmission probability over some baseline schemes in the general region.

Index Terms

Cache, multicast, stochastic geometry, optimization

Y. Cui and D. Jiang are with the Department of Electronic Engineering, Shanghai Jiao Tong University, China. Y. Wu is with the Department of Electrical and Electronic Engineering, The University of Hong Kong, Hong Kong. This paper was presented in part at IEEE GLOBECOM 2015 [1]. Y. Cui was supported in part by the National Science Foundation of China grant 61401272.

I. INTRODUCTION

The demand for wireless communication services has been shifting from connection-oriented services such as traditional voice telephony and messaging to content-oriented services such as multimedia, social networking and smartphone applications. Recently, to support the dramatic growth of wireless data traffic, caching at base stations (BSs) has been proposed as a promising approach for massive content delivery by reducing the distance between popular contents and their requesters (i.e., users) [2]–[4]. In [5]–[7], optimal caching designs are considered for simple models of wireless networks, where channel fading is not considered. For example, in [5], the authors consider the optimal caching and delivery design to minimize the link capacity required to sustain a certain request process in a 2-D square grid network. The combinatorial optimization problem is reduced to a simpler continuous optimization problem with the same order of performance as the original problem. In [6], the authors consider the optimal caching design to minimize the expected file downloading time in a helper-enabled cellular network modeled by a bipartite graph. The optimization problem for the uncoded case is NP-hard, and a greedy caching design is proposed to achieve performance within a factor 2 of the optimum. In [7], the authors consider the optimal caching and routing design in a small cell network. The optimization problem is NP-hard, and a novel reduction to a variant of the facility location problem is proposed to obtain a caching design with approximation guarantees.

In [8]–[11], more realistic network models based on stochastic geometry are considered to characterize the stochastic natures of channel fading and geographic locations of BSs and users. Based on these models, the performance of caching designs at BSs is analyzed and optimized. Specifically, in [8], the authors consider identical caching at BSs (i.e., all BSs store the same set of popular files), and analyze the outage probability and average rate. In [9], the authors consider random caching at BSs, and analyze and optimize the hit probability. In [10], the authors consider random caching in D2D networks, and analyze and optimize the total coverage probability, assuming that content requests follow Zipf distribution. In [11], the authors consider random caching of a uniform distribution, and analyze the cache hit probability and the content outage probability, assuming that content requests follow a uniform distribution. In addition, in [12] and [13], the authors also model cache-enabled wireless networks using stochastic geometry without capturing channel fading (in the performance metrics). Specifically, [12] studies the expected costs of obtaining a complete content under

random uncoded caching and coded caching strategies, which are designed only for different pieces of a single content. Reference [13] considers random caching with contents being stored at each BS in an i.i.d. manner, and analyzes the minimum offloading loss, assuming unknown file popularity profiles. Note that the identical caching design in [8] cannot provide file diversity at different BSs, and hence may not sufficiently exploit storage resources. In contrast, the random caching designs in [9]–[13] can provide file diversity. However, the i.i.d. random caching in [13] may still waste storage resources, as multiple copies of a file may be stored at each BS. The random caching designs in [10]–[12] only provide caching probabilities of files and do not specify how multiple different files can be efficiently stored at each BS based on these probabilities. In [9], the authors provide a graphical method to obtain caching probabilities of file combinations based on the caching probabilities of files, which may not be systematic for large-scale networks. In addition, in [8]–[13], transmission schemes for cached files are not specified. The performance metrics are only related to the coverage probability, and do not reflect resource sharing among users.

On the other hand, enabling multicast service at BSs is an efficient way to deliver popular contents to multiple requesters simultaneously by effectively utilizing the broadcast nature of the wireless medium [14]. Caching and multicasting at BSs have been jointly considered in the literature. For example, in [15], the authors propose a heuristic caching algorithm for a given multicasting design to reduce the service cost. In [16], the authors propose a joint throughput-optimal caching and multicasting algorithm to maximize the service rate. In [17], the authors obtain the optimal dynamic multicast scheduling to minimize the system cost. Note that [15]–[17] focus on algorithm design instead of performance analysis, and do not offer many insights into the fundamental impact of caching and multicasting. In addition, [15]–[17] consider simple network models which cannot capture the geographic features of the locations of BSs and users or statistical properties of signal and interference.

In summary, further studies are required to understand the impact of caching and multicasting in cache-enabled wireless networks. In this paper, we consider the analysis and optimization of joint caching and multicasting in a large-scale wireless network. Our network model effectively characterizes the stochastic natures of channel fading and geographic locations of BSs and users. The main contributions of this paper are summarized below.

- First, we propose a random caching and multicasting scheme with a design parameter to effectively improve the efficiency of information dissemination. Different from [8]–[13],

we specify a transmission scheme, i.e., multicasting, which exploits the broadcast nature of the wireless medium. In addition, different from the random caching designs in [9]–[13], the proposed random caching design is on the basis of file combinations, and can make better use of storage resources when multicasting is considered.

- Next, we analyze the successful transmission probability. Caching on the basis of file combinations significantly complicates the distributions of user associations and interferers, and hence makes the analysis very challenging. By carefully handling different types of interferers and adopting appropriate approximations, we derive a tractable expression for the successful transmission probability in the general region, utilizing tools from stochastic geometry. We also derive a closed-form expression for the successful transmission probability in the high SNR and user density region.¹ These expressions reveal the impacts of physical layer and information-related parameters on the successful transmission probability.

- Then, we consider the successful transmission probability maximization, which is a very complex non-convex problem in general, due to the sophisticated structure of the successful transmission probability. Using optimization techniques, we develop an iterative numerical algorithm to obtain a local optimal caching and multicasting design in the general region. To reduce complexity and maintain superior performance, we derive an asymptotically optimal caching and multicasting design in the high SNR and user density region, based on a two-step optimization framework. The features of the asymptotically optimal design provide important design insights.

- Finally, by numerical simulations, we show that the asymptotically optimal design has much lower computational complexity than the local optimal design and achieves a significant gain in successful transmission probability in the general region over some baseline schemes.

II. SYSTEM MODEL

A. Network Model

We consider a large-scale network, as shown in Fig. 1. The locations of the base stations (BSs) are spatially distributed as a homogeneous Poisson point process (PPP) Φ_b with density λ_b . The locations of the users are distributed as an independent homogeneous PPP with

¹Note that the tractable expression involves integrals, but can be easily computed using numerical computation tools, e.g., MATLAB. The closed-form expression does not have unsolvable integrals, and can be computed much more efficiently.

density λ_u . We consider the downlink transmission. Each BS has one transmit antenna with transmission power P . Each user has one receive antenna. The total bandwidth is W (Hz). Consider a discrete-time system with time being slotted and study one slot of the network. We consider both large-scale fading and small-scale fading. Specifically, due to large-scale fading, transmitted signals with distance D are attenuated by a factor $D^{-\alpha}$, where $\alpha > 2$ is the path loss exponent. For small-scale fading, we assume Rayleigh fading, i.e., each small-scale channel $h \stackrel{d}{\sim} \mathcal{CN}(0, 1)$ or channel power $|h|^2 \stackrel{d}{\sim} \text{Exp}(1)$ [18].²

Let $\mathcal{N} \triangleq \{1, 2, \dots, N\}$ denote the set of $N \geq 1$ files (contents) in the network. For ease of illustration, we assume that all files have the same size.³ Each file is of certain popularity. We assume that the file popularity distribution is identical among all users. Each user randomly requests one file, which is file $n \in \mathcal{N}$ with probability $a_n \in (0, 1]$, where $\sum_{n \in \mathcal{N}} a_n = 1$. Thus, the file popularity distribution is given by $\mathbf{a} \triangleq (a_n)_{n \in \mathcal{N}}$, which is assumed to be known a priori. In addition, without loss of generality (w.l.o.g.), we assume $a_1 \geq a_2 \dots \geq a_N$, i.e., the popularity rank of file n is n .

The network consists of cache-enabled BSs. In particular, each BS is equipped with a cache of size $K \leq N$, storing K different popular files out of N , as illustrated in Fig. 1.⁴ We say every K different files form a combination. Thus, there are $I \triangleq \binom{N}{K}$ different combinations of K different files in total. Let $\mathcal{I} \triangleq \{1, 2, \dots, I\}$ denote the set of I combinations. Combination $i \in \mathcal{I}$ can be characterized by an N -dimensional vector $\mathbf{x}_i \triangleq (x_{i,n})_{n \in \mathcal{N}}$, where $x_{i,n} = 1$ indicates that file n is included in combination i and $x_{i,n} = 0$ otherwise. Note that there are K 1's in each \mathbf{x}_i . Denote $\mathcal{N}_i \triangleq \{n : x_{i,n} = 1\}$ as the set of K files contained in combination i . Note that in practical networks with large N and K , it may not be possible to enumerate all the combinations in \mathcal{I} . However, to understand the natures of joint caching and multicasting in cache-enabled wireless networks, in this paper, we shall first pose the analysis and optimization on the basis of all the file combinations in \mathcal{I} . Then, based on the insights obtained, we shall focus on reducing complexity while maintaining superior performance.

²Rayleigh fading is a widely used probabilistic channel model in existing literature [19], [20]. It is based on the assumption that there are a large number of statistically independent reflected and scattered paths with random amplitudes and random phases uniformly distributed in $[0, 2\pi]$, and *Central Limit Theorem* [18].

³Note that files of different sizes can be divided into chunks of the same length. Thus, the results in this paper can be extended to the case of different file sizes.

⁴Note that storing more than one copies of the same file at one BS is redundant and will waste storage resources.

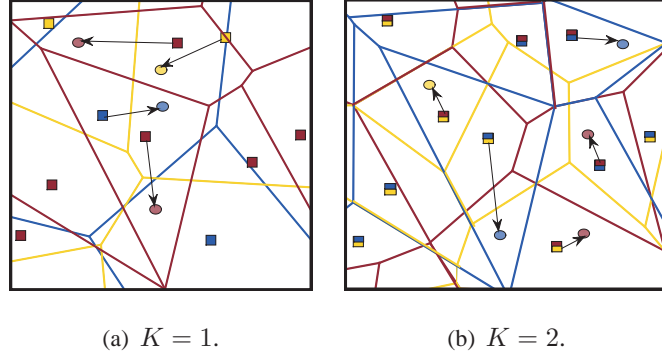


Fig. 1. System model. There are three files ($N = 3$) in the network, represented by the red, yellow and blue colors, respectively. Each circle represents a user, the color of which indicates the file requested by the user. Each square represents a BS, the color of which indicates the file ($K = 1$) or the two different files ($K = 2$) stored at the BS. For each file, there is a corresponding Voronoi tessellation in the same color, which is determined by the locations of the BSs storing this file. Each arrow represents a signal.

B. Caching and Multicasting

We consider random caching on the basis of file combinations. Each BS stores one combination at random, which is combination $i \in \mathcal{I}$ with probability p_i satisfying

$$0 \leq p_i \leq 1, \quad i \in \mathcal{I}, \quad (1)$$

$$\sum_{i \in \mathcal{I}} p_i = 1. \quad (2)$$

A random caching design is specified by the caching distribution $\mathbf{p} \triangleq (p_i)_{i \in \mathcal{I}}$. Let $\mathcal{I}_n \triangleq \{i \in \mathcal{I} : x_{i,n} = 1\}$ denote the set of $I_n \triangleq \binom{N-1}{K-1}$ combinations containing file n . Let

$$T_n \triangleq \sum_{i \in \mathcal{I}_n} p_i, \quad n \in \mathcal{N} \quad (3)$$

denote the probability that file n is stored at a BS. Note that $T_n = p_n$ when $K = 1$. In this paper, we focus on serving cached files at BSs to get the first-order insights into the design of cache-enabled wireless networks, as in [9], [10]. BSs may serve uncached files through other service mechanisms.⁵ The investigation of service mechanisms for uncached files is beyond the scope of this paper.

⁵For example, BSs can fetch some uncached files from the core network through backhaul links and multicast them over other reserved frequency bands. The service of uncached files may involve backhaul cost or extra delay.

As illustrated in Fig. 1, each user requesting file n is associated with the nearest BS storing a combination $i \in \mathcal{I}_n$, referred to as its serving BS, as this BS offers the maximum long-term average receive power for file n [19], [20]. Note that the serving BS of a user may not be its geographically nearest BS and is also statistically determined by the caching distribution \mathbf{p} . We refer to this association mechanism as the *information-centric association*. Different from the traditional *connection-based association* [19], [20], this association jointly considers the physical layer and information-centric properties.

We adopt multicast service⁶ in the cache-enabled wireless network for efficient information dissemination. Consider one BS which has $L_0 \in \{1, 2, \dots\}$ associated users and $K_0 \in \{1, 2, \dots, K\}$ different file requests for the K files stored at this BS. Note that $L_0 \geq K_0$. Under the proposed multicasting transmission scheme, the BS transmits each of the K_0 files at rate τ (bits/second) and over $\frac{1}{K_0}$ of the total bandwidth W (using FDMA). All the users which request one of the K_0 files from this BS try to decode the file from the single multicast transmission of the file at the BS. In contrast, under the traditional connection-based transmission (unicast) scheme, the BS transmits one file to each of the L_0 users at some rate depending on the channel condition and over $\frac{1}{L_0}$ of the total bandwidth W (using FDMA). Note that in this case, $L_0 - K_0$ out of L_0 file transmissions are redundant. Therefore, compared with the traditional connection-based transmission (unicast), this information-centric transmission (multicast) can improve the efficiency of the utilization of the wireless medium and reduce the load of the wireless links.

III. PERFORMANCE METRIC AND PROBLEM FORMULATION

A. Performance Metric

In this paper, w.l.o.g., we study the performance of the typical user denoted as u_0 , which is located at the origin. The index of the typical user and its serving BS is denoted as 0. We assume all BSs are active. According to the caching and user association illustrated in Section II-B, when u_0 requests file n , the received signal of u_0 is given by

$$y_0 = D_{0,0}^{-\frac{\alpha}{2}} h_{0,0} x_0 + \sum_{\ell \in \Phi_b \setminus B_{n,0}} D_{\ell,0}^{-\frac{\alpha}{2}} h_{\ell,0} x_\ell + n_0, \quad (4)$$

⁶Note that in this paper the multicast service happens once every slot, and hence no additional delay is introduced compared with the traditional unicast scheme.

where $B_{n,0}$ is the serving BS of u_0 , $D_{0,0}$ is the distance between u_0 and $B_{n,0}$, $h_{0,0} \stackrel{d}{\sim} \mathcal{CN}(0, 1)$ is the small-scale channel between $B_{n,0}$ and u_0 , x_0 is the transmit signal from $B_{n,0}$ to u_0 , $D_{\ell,0}$ is the distance between BS ℓ and u_0 , $h_{\ell,0} \stackrel{d}{\sim} \mathcal{CN}(0, 1)$ is the small-scale channel between BS ℓ and u_0 , x_ℓ is the transmit signal from BS ℓ to its scheduled user, and $n_0 \stackrel{d}{\sim} \mathcal{CN}(0, N_0)$ is the complex additive white Gaussian noise of power N_0 . The signal-to-interference plus noise ratio (SINR) of u_0 is given by

$$\text{SINR}_{n,0} = \frac{D_{0,0}^{-\alpha} |h_{0,0}|^2}{\sum_{\ell \in \Phi_b \setminus B_{n,0}} D_{\ell,0}^{-\alpha} |h_{\ell,0}|^2 + \frac{N_0}{P}}. \quad (5)$$

In addition, let $K_{n,0} \in \{1, \dots, K\}$ denote the number of different files requested by the users associated with $B_{n,0}$, indicating the file load of $B_{n,0}$. Note that when $K = 1$, $K_{n,0} = 1$; when $K > 1$, $K_{n,0}$ is a discrete random variable, the probability mass function (p.m.f.) of which depends on the user density λ_u . Under the proposed multicasting scheme, each of the $K_{n,0}$ requested files is sent over bandwidth $\frac{W}{K_{n,0}}$ to all the users associated with $B_{n,0}$ and requesting this file. Thus, the corresponding channel capacity of u_0 is given by $C_{n,K,0} \triangleq \frac{W}{K_{n,0}} \log_2(1 + \text{SINR}_{n,0})$. The dissemination of file n at rate τ can be decoded correctly at u_0 if $C_{n,K,0} \geq \tau$. Then, the successful transmission probability of file n requested by u_0 is given by

$$q_{K,n}(\mathbf{p}) \triangleq \Pr[C_{n,K,0} \geq \tau] = \Pr\left[\frac{W}{K_{n,0}} \log_2(1 + \text{SINR}_{n,0}) \geq \tau\right]. \quad (6)$$

Please note that the distributions of random variables $K_{n,0}$ and $\text{SINR}_{n,0}$ depend on \mathbf{p} . Later, we shall see the dependence in the analysis of these distributions. Thus, we write the successful transmission probability of file n requested by u_0 as a function of \mathbf{p} . Requesters are mostly concerned with whether their desired files can be successfully received. Therefore, in this paper, we consider the successful transmission probability of a file requested by u_0 , also referred to as successful transmission probability, as the network performance metric. According to total probability theorem, the successful transmission probability under the proposed multicasting scheme is given by⁷

$$q_K(\mathbf{p}) \triangleq \sum_{n \in \mathcal{N}} a_n q_{K,n}(\mathbf{p}) = \sum_{n \in \mathcal{N}} a_n \Pr\left[\frac{W}{K_{n,0}} \log_2(1 + \text{SINR}_{n,0}) \geq \tau\right]. \quad (7)$$

⁷Note that the traditional SINR coverage probability (which does not capture resource sharing) and rate coverage probability (which only captures resource sharing among different users) cannot reflect resource sharing among different files under the multicasting scheme, and hence are not suitable to measure the performance in our case.

Note that we also write $q_K(\mathbf{p})$ as a function of \mathbf{p} , as $q_{K,n}(\mathbf{p})$ is a function of \mathbf{p} .

Under the proposed caching and multicasting scheme for content-oriented services in the cache-enabled wireless network, the successful transmission probability is sufficiently different from the traditional rate coverage probability studied for connection-oriented services [20]. In particular, the successful transmission probability considered in this paper not only depends on the physical layer parameters, such as the BS density λ_b , user density λ_u , path loss exponent α , bandwidth W and transmit signal-to-noise ratio (SNR) $\frac{P}{N_0}$, but also relies on the information-related parameters, such as the popularity distribution \mathbf{a} , the cache size K and the caching distribution \mathbf{p} . While, the traditional rate coverage probability only depends on the physical layer parameters. In addition, the successful transmission probability depends on the physical layer parameters in a different way from the traditional rate coverage probability. For example, the information-centric association leads to different distributions of the locations of serving and interfering BSs; the multicasting transmission results in different file load distributions at each BS [20]; and the cache-enabled architecture makes the content availability related to the BS density. Later, in Sections IV-A and V-A, we shall analyze the successful transmission probability under the proposed caching and multicasting scheme, i.e., (7), for the unit cache size ($K = 1$) and the general cache size ($K > 1$), respectively.

To further illustrate the advantage of the proposed multicasting scheme over the traditional unicasting scheme for content-oriented services, we also introduce the rate coverage probability under the traditional unicasting scheme for content-oriented services.⁸ Let $L_{n,0} \in \{1, 2, \dots\}$ denote the number of users associated with $B_{n,0}$. Note that $L_{n,0} \geq K_{n,0}$ is a discrete random variable, indicating the user load of $B_{n,0}$. Under the traditional unicasting scheme, each of the $L_{n,0}$ users is served over bandwidth $\frac{W}{L_{n,0}}$ separately. Similarly, the rate coverage probability under the traditional unicasting scheme is given by⁹

$$q_K^{uc}(\mathbf{p}) = \sum_{n \in \mathcal{N}} a_n \Pr \left[\frac{W}{L_{n,0}} \log_2 (1 + \text{SINR}_{n,0}) \geq \tau \right]. \quad (8)$$

⁸Note that in this paper, for the tractability of the analysis and obtaining first-order design insights, we assume that all the files are delivered at the same rate τ . Under this assumption, there is no intricate tradeoff between unicast and multicast. We would like to consider content transmissions at multiple bit rates and multicast grouping in future work.

⁹Note that $q_K^{uc}(\mathbf{p})$ is for content-oriented services in a cache-enabled network and is still different from the traditional rate coverage probability for connection-oriented services [20]. The purpose of introducing $q_K^{uc}(\mathbf{p})$ is for demonstrating the gain of multicasting over unicasting. We will not analyze or optimize $q_K^{uc}(\mathbf{p})$ in (8).

where τ can be interpreted as the rate threshold. Similarly, please note that the distributions of random variables $L_{n,0}$ and $\text{SINR}_{n,0}$ depend on \mathbf{p} . Thus, we also write $q_K^{uc}(\mathbf{p})$ as a function of \mathbf{p} . Since the file load is smaller than or equal to the user load, i.e., $K_{n,0} \leq L_{n,0}$ with probability one, we can easily conclude $q_K(\mathbf{p}) > q_K^{uc}(\mathbf{p})$, for any given caching distribution \mathbf{p} . In addition, as the user density λ_u increases, $q_K(\mathbf{p}) - q_K^{uc}(\mathbf{p})$ increases. This illustrates the advantage of the proposed multicasting scheme over the traditional unicasting scheme for content-oriented services, especially in the high user density region. Later, we shall evaluate $q_K^{uc}(\mathbf{p})$ in (8) numerically to demonstrate this advantage.

B. Problem Formulation

The caching and multicasting design fundamentally affects the network performance via the caching distribution \mathbf{p} . We would like to consider the optimal caching and multicasting to maximize the successful transmission probability by carefully optimizing the design parameter \mathbf{p} . Specifically, we consider the following optimization problem.

Problem 1 (Caching and Multicasting Optimization):

$$\begin{aligned} \max_{\mathbf{p}} \quad & q_K(\mathbf{p}) \\ \text{s.t.} \quad & (1), (2), \end{aligned}$$

where $q_K(\mathbf{p})$ is given by (7).

Note that in this paper, we focus on the successful transmission probability maximization to get first-order insights into the design of cache-enabled wireless networks.¹⁰ The optimization framework in this paper can be easily applied to address the QoS requirements in terms of the successful transmission probability of each file, e.g., $q_{K,n}(\mathbf{p}) \geq Q_{K,n}$ for all $n \in \mathcal{N}$. Later, in Sections IV-B and V-B, we shall solve Problem 1 for the unit cache size ($K = 1$) and the general cache size ($K > 1$), respectively.

IV. ANALYSIS AND OPTIMIZATION FOR UNIT CACHE SIZE

In this section, we consider the unit cache size, i.e., $K = 1$. In this case, each combination contains only one file, and there are only $I = N$ combinations. Therefore, when $K = 1$, for

¹⁰The optimal solution to Problem 1 may result in starvation of requesters for files with low caching probabilities. We assume these starving users can be satisfied through other service mechanisms at additional backhaul or delay costs.

ease of illustration, we use the file index $n \in \mathcal{N}$ instead of the combination index $i \in \mathcal{I}$, and write the caching distribution as $\mathbf{p} = (p_n)_{n \in \mathcal{N}}$. In addition, we have $K_{n,0} = 1$. In the following, we first analyze the successful transmission probability for a given design parameter \mathbf{p} . Then, we optimize the design parameter \mathbf{p} to maximize the successful transmission probability.

A. Performance Analysis

In this part, we analyze the successful transmission probability for given \mathbf{p} when $K = 1$. Note that different from the traditional connection-based network, in the cache-enabled wireless network considered in this paper, there are two types of interferers, namely, i) interfering BSs storing the file requested by u_0 (these BSs are further than the serving BS of u_0), and ii) interfering BSs storing the other files (these BSs could be closer to u_0 than the serving BS of u_0). By carefully handling these two types of interferers, we obtain $q_{1,n}(\mathbf{p})$ using stochastic geometry. Substituting $q_{1,n}(\mathbf{p})$ into (7), we have the following result.

Theorem 1 (Performance for $K = 1$): The successful transmission probability $q_1(\mathbf{p})$ of u_0 is given by

$$q_1(\mathbf{p}) = \sum_{n \in \mathcal{N}} a_n f_1(p_n), \quad (9)$$

where

$$\begin{aligned} f_k(x) \triangleq & 2\pi\lambda_b x \int_0^\infty d \exp\left(-\frac{2\pi}{\alpha} x \lambda_b \left(2^{\frac{k\tau}{W}} - 1\right)^\frac{2}{\alpha} d^2 B'\left(\frac{2}{\alpha}, 1 - \frac{2}{\alpha}, 2^{-\frac{k\tau}{W}}\right)\right) \\ & \times \exp(-\pi\lambda_b x d^2) \exp\left(-\left(2^{\frac{k\tau}{W}} - 1\right) d^\alpha \frac{N_0}{P}\right) \\ & \times \exp\left(-\frac{2\pi}{\alpha} (1-x) \lambda_b \left(2^{\frac{k\tau}{W}} - 1\right)^\frac{2}{\alpha} d^2 B\left(\frac{2}{\alpha}, 1 - \frac{2}{\alpha}\right)\right) dd. \end{aligned} \quad (10)$$

Here, $B'(x, y, z) \triangleq \int_z^1 u^{x-1} (1-u)^{y-1} du$ is the complementary incomplete Beta function, and $B(x, y) \triangleq \int_0^1 u^{x-1} (1-u)^{y-1} du$ is the Beta function.

Proof: Please refer to Appendix A. ■

From Theorem 1, we can see that in the general region, the physical layer parameters α , W , λ_b , $\frac{P}{N_0}$ and the caching distribution \mathbf{p} jointly affect the successful transmission probability $q_1(\mathbf{p})$. The impacts of the physical layer parameters and the caching distribution on $q_1(\mathbf{p})$ are coupled in a complex manner.

The successful transmission probability $q_1(\mathbf{p})$ increases with the transmit SNR $\frac{P}{N_0}$. From Theorem 1, we have the following corollary.

Corollary 1 (Asymptotic Performance for $K = 1$): When $\frac{P}{N_0} \rightarrow \infty$, the successful transmission probability of u_0 is given by

$$q_{1,\infty}(\mathbf{p}) \triangleq \lim_{\frac{P}{N_0} \rightarrow \infty} q_1(\mathbf{p}) = \sum_{n \in \mathcal{N}} \frac{a_n p_n}{c_{2,1} + c_{1,1} p_n}, \quad (11)$$

where

$$c_{1,k} \triangleq 1 + \frac{2}{\alpha} \left(2^{\frac{k\tau}{W}} - 1\right)^{\frac{2}{\alpha}} B' \left(\frac{2}{\alpha}, 1 - \frac{2}{\alpha}, 2^{-\frac{k\tau}{W}}\right) - \frac{2}{\alpha} \left(2^{\frac{k\tau}{W}} - 1\right)^{\frac{2}{\alpha}} B \left(\frac{2}{\alpha}, 1 - \frac{2}{\alpha}\right), \quad (12)$$

$$c_{2,k} \triangleq \frac{2}{\alpha} \left(2^{\frac{k\tau}{W}} - 1\right)^{\frac{2}{\alpha}} B \left(\frac{2}{\alpha}, 1 - \frac{2}{\alpha}\right). \quad (13)$$

Proof: Please refer to Appendix B. ■

From Corollary 1, we can see that in the high SNR region, the impact of the physical layer parameters α and W , captured by $c_{1,1}$ and $c_{2,1}$, and the impact of the caching distribution \mathbf{p} on $q_{1,\infty}(\mathbf{p})$ can be easily separated. Later, in Section IV-B, we shall see that this separation greatly facilitates the optimization of $q_{1,\infty}(\mathbf{p})$ over \mathbf{p} .

Fig. 2 plots the successful transmission probability versus the transmit SNR $\frac{P}{N_0}$. From Fig. 2, we can see that the analytical curve for the general transmit SNR is very close to the Monte Carlo curve. In addition, we can see that the analytical curve for the general transmit SNR asymptotically approaches the analytical curve for the asymptotic transmit SNR. These observations verify Theorem 1 and Corollary 1, respectively. From Fig. 2, we can also observe that $q_{1,\infty}(\mathbf{p})$ provides a simple and good approximation for $q_1(\mathbf{p})$ in the high transmit SNR region (e.g., $\frac{P}{N_0} \geq 40$ dB). On the other hand, Fig. 2 shows that $q_1(\mathbf{p})$, which does not depend on user density λ_u (when $K = 1$), is greater than $q_1^{uc}(\mathbf{p})$, which depends on the user density λ_u , as discussed in Section III-A. This demonstrates the advantage of the proposed multicasting scheme over the traditional unicasting scheme.

B. Performance Optimization

In this part, we study the successful transmission probability optimization in Problem 1 for $K = 1$, with $q_1(\mathbf{p})$ in (9) being the objective function. In general, it is difficult to ensure the convexity of $q_1(\mathbf{p})$, as it is in a very complex form. On the other hand, $q_1(\mathbf{p})$ is differentiable, and the constraints in (1) and (2) are linear. Thus, Problem 1 for $K = 1$ is an optimization of a differentiable (non-convex) function over a convex set. A local optimal solution can be

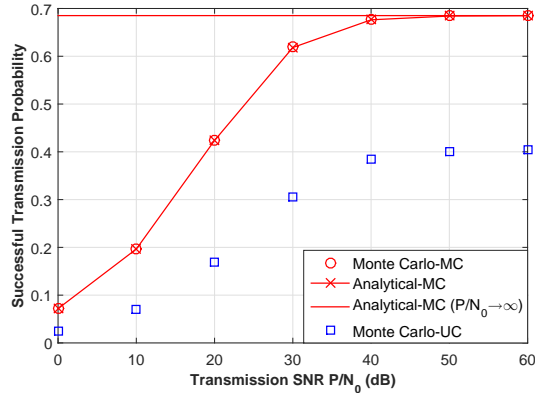


Fig. 2. Successful transmission probability versus transmit SNR $\frac{P}{N_0}$ at $K = 1$. $\lambda_b = 0.01$, $\lambda_u = 0.1$, $\alpha = 4$, $W = 10 \times 10^6$, $\tau = 5 \times 10^5$, $N = 5$, $\mathbf{p} = (0.6811, 0.3189, 0, 0, 0)$, and $a_n = \frac{n^{-\gamma}}{\sum_{n \in \mathcal{N}} n^{-\gamma}}$ with $\gamma = 2$. MC stands for multicast, while UC stands for unicast. In this paper, to simulate the large-scale network, we use a 2-dimensional square of area 260^2 , which is sufficiently large in our case. Note that if the simulation window size is not large enough, the observed interference would be smaller than the true interference due to the edge effect, resulting in larger successful transmission probability than the true value. In addition, the Monte Carlo results are obtained by averaging over 4×10^6 random realizations.

Algorithm 1 Local Optimal Solution for $K = 1$

- 1: Initialize $t = 1$ and $p_n(1) = \frac{1}{N}$ for all $n \in \mathcal{N}$.
 - 2: For all $n \in \mathcal{N}$, compute $\bar{p}_n(t+1)$ according to $\bar{p}_n(t+1) = p_n(t) + \epsilon(t) \frac{\partial q_1(\mathbf{p}(t))}{\partial p_n(t)}$, where $\{\epsilon(t)\}$ satisfies (14).
 - 3: For all $n \in \mathcal{N}$, compute $p_n(t+1)$ according to $p_n(t+1) = \min \{[\bar{p}_n(t+1) - \nu^*]^+, 1\}$, where ν^* satisfies $\sum_{n \in \mathcal{N}} \min \{[\bar{p}_n(t+1) - \nu^*]^+, 1\} = 1$.
 - 4: Set $t = t + 1$ and go to Step 2.
-

obtained using standard gradient projection methods [21, pp. 223]. Here, we consider the diminishing stepsize [21, pp. 227] satisfying

$$\epsilon(t) \rightarrow 0 \text{ as } t \rightarrow \infty, \quad \sum_{t=1}^{\infty} \epsilon(t) = \infty, \quad \sum_{t=1}^{\infty} \epsilon(t)^2 < \infty, \quad (14)$$

and propose Algorithm 1 to obtain a local optimal solution. It is shown in [21, pp. 229] that $\mathbf{p}(t) \rightarrow \mathbf{p}^\dagger$ as $t \rightarrow \infty$, where \mathbf{p}^\dagger is a local optimal solution to Problem 1 for $K = 1$.

In Step 2 of Algorithm 1, $\frac{\partial q_1(\mathbf{p}(t))}{\partial p_n(t)} = a_n f'_1(p_n)$, where

$$\begin{aligned}
f'_k(x) = & \frac{f_k(x)}{x} + 2\pi\lambda_b x \int_0^\infty d \exp\left(-\frac{2\pi}{\alpha} x \lambda_b \left(2^{\frac{k\tau}{W}} - 1\right)^{\frac{2}{\alpha}} d^2 B' \left(\frac{2}{\alpha}, 1 - \frac{2}{\alpha}, 2^{-\frac{k\tau}{W}}\right)\right) \\
& \times \exp(-\pi\lambda_b x d^2) \exp\left(-\left(2^{\frac{k\tau}{W}} - 1\right) d^\alpha \frac{N_0}{P}\right) \\
& \times \exp\left(-\frac{2\pi}{\alpha} (1-x) \lambda_b \left(2^{\frac{k\tau}{W}} - 1\right)^{\frac{2}{\alpha}} d^2 B \left(\frac{2}{\alpha}, 1 - \frac{2}{\alpha}\right)\right) \\
& \times \left(-\frac{2\pi}{\alpha} \lambda_b \left(2^{\frac{k\tau}{W}} - 1\right)^{\frac{2}{\alpha}} d^2 B' \left(\frac{2}{\alpha}, 1 - \frac{2}{\alpha}, 2^{-\frac{k\tau}{W}}\right) - \pi\lambda_b d^2\right. \\
& \left. + \frac{2\pi}{\alpha} \lambda_b \left(2^{\frac{k\tau}{W}} - 1\right)^{\frac{2}{\alpha}} d^2 B \left(\frac{2}{\alpha}, 1 - \frac{2}{\alpha}\right)\right) dd. \tag{15}
\end{aligned}$$

Note that Step 3 of Algorithm 1 is the projection of $\bar{\mathbf{p}}_n(t+1)$ onto the set of the variables satisfying the constraints in (1) and (2). In other words, $p_n(t+1)$ given in Step 3 is the solution to the following optimization problem [21, pp. 201].¹¹

$$\begin{aligned}
\min_{\mathbf{p}} \quad & \|\mathbf{p} - \bar{\mathbf{p}}(t+1)\|^2 \\
s.t. \quad & (1), (2).
\end{aligned}$$

Here, $\|\cdot\|$ denotes the Euclidean norm.

As computing the gradient of $q_1(\mathbf{p})$ in each iteration involves very high complexity, Algorithm 1 may not be suitable for this problem when N is large. Therefore, instead, we focus on obtaining an asymptotically (global) optimal solution when $\frac{P}{N_0} \rightarrow \infty$. Specifically, we consider the optimization of the asymptotic successful transmission probability, i.e., Problem 1 with $q_{1,\infty}(\mathbf{p})$ in (11) being the objective function.

Problem 2 (Asymptotic Optimization for $K = 1$):

$$\begin{aligned}
\max_{\mathbf{p}} \quad & q_{1,\infty}(\mathbf{p}) \\
s.t. \quad & (1), (2).
\end{aligned}$$

The optimal solution $\mathbf{p}^* \triangleq (p_n^*)_{n \in \mathcal{N}}$ to Problem 2 is an asymptotically optimal solution to Problem 1 for $K = 1$, and the resulting successful transmission probability $q_{1,\infty}^* \triangleq q_{1,\infty}(\mathbf{p}^*)$ is the asymptotically optimal successful transmission probability to Problem 1 for $K = 1$. In the following, we focus on solving Problem 2 to obtain an asymptotically optimal solution to Problem 1 for $K = 1$.

¹¹This can be easily shown using KKT conditions. We omit the details due to page limitation.

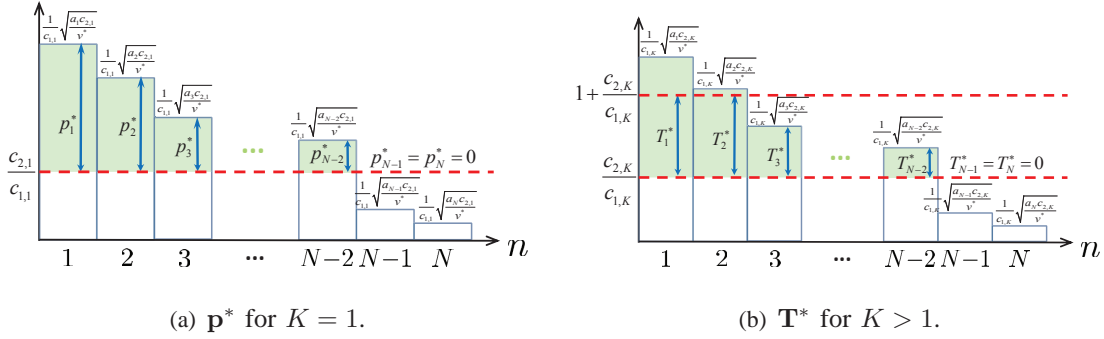


Fig. 3. Illustration of the optimality structure.

It can be easily seen that Problem 2 is convex and Slater's condition is satisfied, implying that strong duality holds. Using KKT conditions, we can solve Problem 2.

Theorem 2 (Asymptotically Optimal Solution for $K = 1$): An asymptotically optimal solution $\mathbf{p}^* = (p_n^*)_{n \in \mathcal{N}}$ to Problem 1 for $K = 1$ is given by

$$p_n^* = \left[\frac{1}{c_{1,1}} \sqrt{\frac{a_n c_{2,1}}{\nu^*}} - \frac{c_{2,1}}{c_{1,1}} \right]^+, \quad n \in \mathcal{N}, \quad (16)$$

where $[x]^+ \triangleq \max\{x, 0\}$ and ν^* satisfies

$$\sum_{n \in \mathcal{N}} \left[\frac{1}{c_{1,1}} \sqrt{\frac{a_n c_{2,1}}{\nu^*}} - \frac{c_{2,1}}{c_{1,1}} \right]^+ = 1. \quad (17)$$

Here, $c_{1,1}$ and $c_{2,1}$ are given by (12) and (13), respectively.

Proof: Please refer to Appendix C. ■

Remark 1 (Interpretation of Theorem 2): As illustrated in Fig. 3 (a), the asymptotically optimal solution \mathbf{p}^* given by Theorem 2 has a reverse water-filling structure. The file popularity distribution \mathbf{a} and the physical layer parameters (captured in $c_{1,1}$ and $c_{2,1}$) jointly affect ν^* . Given ν^* , the physical layer parameters (captured in $c_{1,1}$ and $c_{2,1}$) affect the caching probabilities of all the files in the same way, while the popularity of file n (i.e., a_n) only affects the caching probability of file n (i.e., p_n^*). From Theorem 2, we have $p_1^* \geq p_2^* \geq \dots \geq p_N^*$, as $a_1 \geq a_2 \dots \geq a_N$. In other words, files of higher popularity get more storage resources. In addition, there may exist \bar{n} ($1 < \bar{n} < N$) such that $p_n^* > 0$ for all $n < \bar{n}$, and $p_n^* = 0$ for all $n \geq \bar{n}$. In other words, some files of lower popularity may not be stored. For a popularity distribution with a heavy tail, \bar{n} is large, i.e., more different files can be stored.

As the water-level in the traditional water-filling power control, the root ν^* to the equation in (17) can be easily solved. Thus, we can efficiently compute \mathbf{p}^* based on Theorem 2. In

addition, from Theorem 2, we have the following corollary.

Corollary 2 (Asymptotically Optimal Solution for $K = 1$): If $\frac{\sqrt{a_N}}{\sum_{n \in \mathcal{N}} \sqrt{a_n}} > \frac{c_{2,1}}{c_{1,1} + c_{2,1}N}$, then we have

$$p_n^* = \left(1 + \frac{c_{2,1}}{c_{1,1}}N\right) \frac{\sqrt{a_n}}{\sum_{n \in \mathcal{N}} \sqrt{a_n}} - \frac{c_{2,1}}{c_{1,1}} > 0, \quad n \in \mathcal{N}, \quad (18)$$

$$q_{1,\infty}^* = \frac{1}{c_{1,1}} \left(1 - \frac{(\sum_{n \in \mathcal{N}} \sqrt{a_n})^2}{N + \frac{c_{1,1}}{c_{2,1}}}\right). \quad (19)$$

Here, $c_{1,1}$ and $c_{2,1}$ are given by (12) and (13), respectively.

Note that the condition $\frac{\sqrt{a_N}}{\sum_{n \in \mathcal{N}} \sqrt{a_n}} > \frac{c_{2,1}}{c_{1,1} + c_{2,1}N}$ means that the popularity distribution has a relatively heavy tail. Under this condition, all files are stored, and interestingly, the caching probability of file n increases linearly with $\frac{\sqrt{a_n}}{\sum_{n \in \mathcal{N}} \sqrt{a_n}}$ instead of a_n .

V. ANALYSIS AND OPTIMIZATION FOR GENERAL CACHE SIZE

In this section, we consider the general cache size, i.e., $K > 1$. We first analyze the successful transmission probability for a given design parameter \mathbf{p} , by adopting appropriate approximations. Then, we study the maximization of the successful transmission probability over \mathbf{p} .

A. Performance Analysis

In this part, we would like to analyze the successful transmission probability $q_K(\mathbf{p})$ in (7) for a given design parameter \mathbf{p} when $K > 1$. In general, for all $n \in \mathcal{N}$, file load $K_{n,0}$ and SINR $\text{SINR}_{n,0}$ are correlated, as BSs with larger association regions have higher file load and lower SINR (due to larger user to BS distance) [22]. However, the exact relationship between $K_{n,0}$ and $\text{SINR}_{n,0}$ is very complex and is still not known. For the tractability of the analysis, as in [22] and [20], the dependence is ignored. Then, from (7), we have

$$q_K(\mathbf{p}) = \sum_{n \in \mathcal{N}} a_n \sum_{k=1}^K \Pr[K_{n,0} = k] \Pr\left[\frac{W}{k} \log_2(1 + \text{SINR}_{n,0}) \geq \tau\right]. \quad (20)$$

First, we calculate the p.m.f. of random file load $K_{n,0}$. In calculating $\Pr[K_{n,0} = k]$, we need the probability density function (p.d.f.) of the size of the Voronoi cell of $B_{n,0}$ w.r.t. file $m \in \mathcal{N}_{i,-n} \triangleq \mathcal{N}_i \setminus \{n\}$ when $B_{n,0}$ contains combination $i \in \mathcal{I}_n$. However, this p.d.f. is very complex and is still unknown. For the tractability of the analysis, we approximate this p.d.f.

based on a tractable approximated form of the p.d.f. of the size of the Voronoi cell to which a randomly chosen user belongs [23], which is widely used in existing literature [20], [22]. Under this approximation, we calculate the p.m.f. of $K_{n,0}$. The accuracy of the approximation will be demonstrated in Fig. 4 and Table I.

Lemma 1 (p.m.f. of $K_{n,0}$): The p.m.f. of $K_{n,0}$ is given by

$$\Pr[K_{n,0} = k] \approx \sum_{i \in \mathcal{I}_n} \frac{p_i}{T_n} \sum_{\mathcal{N}_i^1 \in \mathcal{SN}_i^1(k-1)} G_{n,i}(\mathcal{N}_i^1, \mathbf{T}_{i,-n}), \quad k = 1, \dots, K, \quad (21)$$

where $\mathcal{SN}_i^1(k-1) \triangleq \{\mathcal{N}_i^1 \subseteq \mathcal{N}_{i,-n} : |\mathcal{N}_i^1| = k-1\}$, $\mathbf{T}_{i,-n} \triangleq (T_m)_{m \in \mathcal{N}_{i,-n}}$, $W_m(T_m) \triangleq 1 + 3.5^{-1} \frac{a_m \lambda_u}{T_m \lambda_b}$ and $G_{n,i}(\mathcal{N}_i^1, \mathbf{T}_{i,-n}) \triangleq \prod_{m \in \mathcal{N}_i^1} (1 - W_m(T_m))^{-4.5} \prod_{m \in \mathcal{N}_{i,-n} \setminus \mathcal{N}_i^1} W_m(T_m)^{-4.5}$.

Proof: Please refer to Appendix D. ■

From Lemma 1, we have the following corollary.

Corollary 3 (p.m.f. of $K_{n,0}$ when $\lambda_u \rightarrow \infty$): When $\lambda_u \rightarrow \infty$, we have

$$\lim_{\lambda_u \rightarrow \infty} \Pr[K_{n,0} = k] = \begin{cases} 0, & k = 1, \dots, K-1 \\ 1, & k = K \end{cases}. \quad (22)$$

By Corollary 3, we know that the (approximated) random variable $K_{n,0} \in \{1, \dots, K\}$ converges to the constant K in distribution, as $\lambda_u \rightarrow \infty$. Note that in the high user density region, the exact file load for each BS turns to K . Thus, Corollary 3 indicates that the approximation error used for obtaining the p.m.f. of $K_{n,0}$ in Lemma 1 is asymptotically negligible.

Next, we calculate $\Pr[\frac{W}{k} \log_2(1 + \text{SINR}_{n,0}) \geq \tau]$. Similar to the case for $K = 1$, there are two types of interferers, namely, i) interfering BSs storing the combinations containing the file requested by u_0 , and ii) interfering BSs without the desired file of u_0 . By carefully handling these two types of interferers, we obtain $\Pr[\frac{W}{k} \log_2(1 + \text{SINR}_{n,0}) \geq \tau] = f_k(T_n)$ using stochastic geometry. Then, based on Lemma 1 and $\Pr[\frac{W}{k} \log_2(1 + \text{SINR}_{n,0}) \geq \tau] = f_k(T_n)$, we can obtain $q_K(\mathbf{p})$ for $K > 1$.

Theorem 3 (Performance for $K > 1$): The successful transmission probability $q_K(\mathbf{p})$ of u_0 is given by

$$q_K(\mathbf{p}) = \sum_{n \in \mathcal{N}} a_n \sum_{k=1}^K \Pr[K_{n,0} = k] f_k(T_n), \quad (23)$$

where $\Pr[K_{n,0} = k]$ is given by Lemma 1, $f_k(T_n)$ is given by (10) and T_n is given by (3).

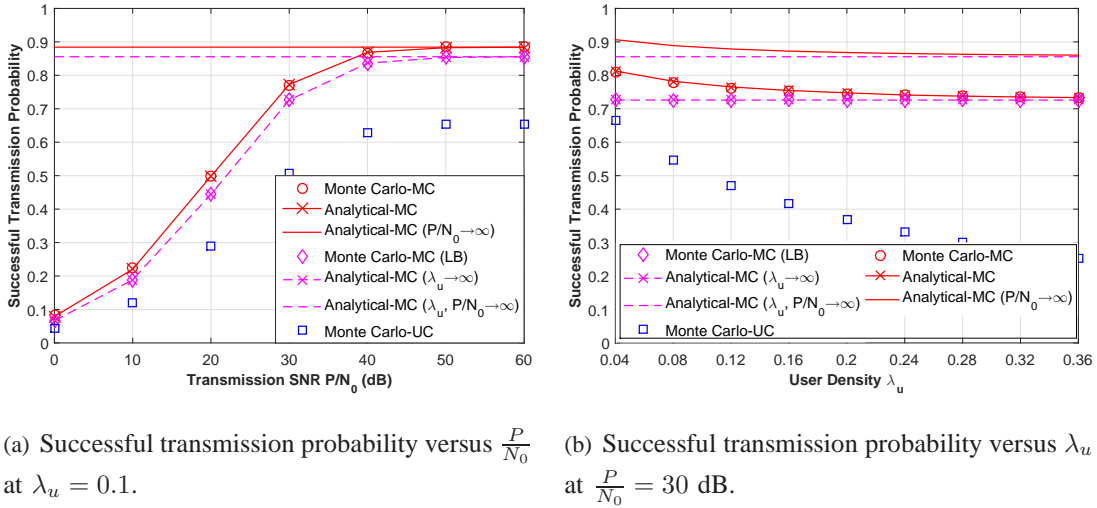


Fig. 4. Successful transmission probability versus transmit SNR $\frac{P}{N_0}$ and user density λ_u at $K = 4$, $\lambda_b = 0.01$, $\alpha = 4$, $W = 10 \times 10^6$, $\tau = 5 \times 10^5$, $N = 5$, $\mathbf{p} = (0.6811, 0.3189, 0, 0, 0)$, and $a_n = \frac{n^{-\gamma}}{\sum_{n \in \mathcal{N}} n^{-\gamma}}$ with $\gamma = 2$. Here, $\mathcal{N}_1 = \{1, 2, 3, 4\}$, $\mathcal{N}_2 = \{1, 2, 3, 5\}$, $\mathcal{N}_3 = \{1, 2, 4, 5\}$, $\mathcal{N}_4 = \{1, 3, 4, 5\}$, and $\mathcal{N}_5 = \{2, 3, 4, 5\}$.

Proof: Please refer to Appendix E. ■

Similarly, from Theorem 3, we can see that in the general region, the physical layer parameters α , W , λ_b , λ_u and $\frac{P}{N_0}$ and the caching distribution \mathbf{p} jointly affect the successful transmission probability $q_K(\mathbf{p})$, by affecting $\Pr[K_{n,0} = k]$ and $f_k(T_n)$ for all $k = 1, \dots, K$. The impacts of the physical layer parameters and the caching distribution on $q_K(\mathbf{p})$ are coupled in a complex manner.

The successful transmission probability $q_K(\mathbf{p})$ increases with $\frac{P}{N_0}$ and decreases with λ_u . From Theorem 3 and Corollary 3, we have the following corollary.

Corollary 4 (Asymptotic Performance for $K > 1$): When $\frac{P}{N_0} \rightarrow \infty$ and $\lambda_u \rightarrow \infty$, the successful transmission probability of u_0 is given by

$$q_{K,\infty}(\mathbf{p}) \triangleq \lim_{\lambda_u \rightarrow \infty, \frac{P}{N_0} \rightarrow \infty} q_K(\mathbf{p}) = \sum_{n \in \mathcal{N}} \frac{a_n T_n}{c_{2,K} + c_{1,K} T_n}. \quad (24)$$

Here, $c_{1,K}$ and $c_{2,K}$ are given by (12) and (13), respectively, and T_n is given by (3).

Proof: Corollary 4 can be proved in a similar way to Corollary 1. We omit the details due to page limitation. ■

Similarly, from Corollary 4, we can see that in the high SNR and user density region, the impact of the physical layer parameters α and W , captured by $c_{1,K}$ and $c_{2,K}$, and the impact of the caching distribution \mathbf{p} on the successful transmission probability $q_{K,\infty}(\mathbf{p})$ can

be easily separated. Later, in Section V-B, we shall see that this separation greatly facilitates the optimization of $q_{K,\infty}(\mathbf{p})$.

Fig. 4 plots the successful transmission probability for $K > 1$ versus the transmit SNR $\frac{P}{N_0}$ and the user density λ_u . Fig. 4 verifies Theorem 3 and Corollary 4, and demonstrates the accuracy of the approximations adopted. Fig. 4 also indicates that $q_{K,\infty}(\mathbf{p})$ provides a simple and good approximation for $q_K(\mathbf{p})$ in the high transmit SNR region (e.g., $\frac{P}{N_0} \geq 40$ dB) and the high user density region (e.g., $\lambda_u \geq 0.16$). On the other hand, Fig. 4 shows that $q_K(\mathbf{p})$ is greater than $q_K^{uc}(\mathbf{p})$; $q_K(\mathbf{p})$ and $q_K^{uc}(\mathbf{p})$ both decrease with λ_u ; and the gap $q_K(\mathbf{p}) - q_K^{uc}(\mathbf{p})$ increases with λ_u . These observations verify the discussions in Section III-A and demonstrate the advantage of the proposed multicasting scheme over the traditional unicasting scheme. Table I further illustrates the approximation error versus the number of files N . From Table I, we can see that under the parameters considered in the simulation, the approximation error is very small, and there is no observable increase of the approximation error with N .

N	200	400	600	800	1000
Monte Carlo-MC	0.5051	0.4822	0.4705	0.4636	0.4582
Analytical-MC	0.5035	0.4803	0.4691	0.4620	0.4568
Approximation Error	0.0016	0.0019	0.0014	0.0016	0.0014
Relative Approximation Error	0.32%	0.39%	0.30%	0.35%	0.31%

TABLE I. Approximation error between the analytical successful transmission probability in Theorem 3 and the numerical successful transmission probability. $W = 10 \times 10^6$, $\tau = 5 \times 10^5$, $\lambda_b = 0.01$, $\lambda_u = 0.1$, $K = 20$,

$$\alpha = 4, \frac{P}{N_0} = 30 \text{ dB}, a_n = \frac{n^{-\gamma}}{\sum_{n \in \mathcal{N}} n^{-\gamma}} \text{ with } \gamma = 1.2, \text{ and } \mathbf{p} = \mathbf{p}^* \text{ given by Problem 5.}$$

B. Performance Optimization

In this part, we consider the successful transmission probability optimization in Problem 1 for $K > 1$, with $q_K(\mathbf{p})$ in (23) being the objective function. Similarly, Problem 1 for $K > 1$ is an optimization of a differentiable (non-convex) function over a convex set. A local optimal solution can be obtained using the standard gradient projection method in Algorithm 2. It is shown in [21, pp. 229] that $\mathbf{p}(t) \rightarrow \mathbf{p}^\dagger$ as $t \rightarrow \infty$, where \mathbf{p}^\dagger is a local optimal solution to Problem 1 for $K > 1$.

Algorithm 2 Local Optimal Solution for $K > 1$

- 1: Initialize $t = 1$ and $p_i(1) = \frac{1}{I}$ for all $i \in \mathcal{I}$.
 - 2: For all $i \in \mathcal{I}$, compute $\bar{p}_i(t+1)$ according to $\bar{p}_i(t+1) = p_i(t) + \epsilon(t) \frac{\partial q_K(\mathbf{p}(t))}{\partial p_i(t)}$, where $\{\epsilon(t)\}$ satisfies (14).
 - 3: For all $i \in \mathcal{I}$, compute $p_i(t+1)$ according to $p_i(t+1) = \min \{[\bar{p}_i(t+1) - \nu^*]^+, 1\}$, where ν^* satisfies $\sum_{i \in \mathcal{I}} \min \{[\bar{p}_i(t+1) - \nu^*]^+, 1\} = 1$.
 - 4: Set $t = t + 1$ and go to Step 2.
-

In Step 2 of Algorithm 2, $\frac{\partial q_K(\mathbf{p}(t))}{\partial p_i(t)}$ is given by

$$\begin{aligned}
\frac{\partial q_K(\mathbf{p})}{\partial p_i} &= \sum_{n \in \mathcal{N}_i} a_n \sum_{k=1}^K \frac{f_k(T_n)}{T_n} \sum_{\mathcal{N}_i^1 \in \mathcal{SN}_i^1(k-1)} G_{n,i}(\mathcal{N}_i^1, \mathbf{T}_{i,-n}) \\
&+ \sum_{m' \in \mathcal{N}} \left(\sum_{n \in \mathcal{N}, n \neq m'} a_n \sum_{k=1}^K \frac{f_k(T_n)}{T_n} \sum_{i' \in \mathcal{I}_n, i' \in \mathcal{I}_{m'}} p_{i'} \frac{4.5 a_{m'} \lambda_u}{3.5 T_{m'}^2 \lambda_b} W_{m'}(T_{m'})^{-1} \right. \\
&\times \left(\sum_{\substack{\mathcal{N}_{i'}^1 \in \mathcal{SN}_{i'}^1(k-1) \\ m' \notin \mathcal{N}_{i'}^1}} G_{n,i'}(\mathcal{N}_{i'}^1, \mathbf{T}_{i',-n}) - \frac{W_{m'}(T_{m'})^{-4.5}}{1 - W_{m'}(T_{m'})^{-4.5}} \sum_{\substack{\mathcal{N}_{i'}^1 \in \mathcal{SN}_{i'}^1(k-1) \\ m' \in \mathcal{N}_{i'}^1}} G_{n,i'}(\mathcal{N}_{i'}^1, \mathbf{T}_{i',-n}) \right) \\
&\left. + a_{m'} \sum_{k=1}^K \frac{f'_k(T_{m'}) T_{m'} - f_k(T_{m'})}{T_{m'}^2} \sum_{i' \in \mathcal{I}_{m'}} p_{i'} \sum_{\mathcal{N}_{i'}^1 \in \mathcal{SN}_{i'}^1(k-1)} G_{m',i'}(\mathcal{N}_{i'}^1, \mathbf{T}_{i',-m'}) \right) \mathbf{1}[i \in \mathcal{I}_{m'}],
\end{aligned} \tag{25}$$

where $\mathbf{1}[\cdot]$ denotes the indicator function and $f'_k(x)$ is given by (15). Step 3 is the projection of $\bar{p}_i(t+1)$ onto the set of the variables satisfying the constraints in (1) and (2).

As there are $I = \binom{N}{K}$ optimization variables $\mathbf{p} = (p_i)_{i \in \mathcal{I}}$ in Problem 1 for $K > 1$ and calculating $\frac{\partial q_K(\mathbf{p}(t))}{\partial p_i(t)}$ for each $i \in \mathcal{I}$ in each iteration involves high complexity (due to the complex form of $q_K(\mathbf{p})$ in (23)), the computational complexity of a local optimal solution using Algorithm 2 is very high for large N . In the following, we propose a two-step optimization framework to obtain an asymptotically optimal solution with manageable complexity and superior performance. Specifically, we first identify a set of asymptotically optimal solutions in the high SNR and user density region, by optimizing $q_{K,\infty}(\mathbf{p})$ in (24) among all feasible solutions. Then, we obtain the asymptotically optimal solution achieving the optimal successful transmission probability in the general region among the set of asymptotically optimal solutions, referred to as the best asymptotically optimal solution, by optimizing

$q_K(\mathbf{p})$ in (23) within this set. Later, in Fig. 5, we shall verify that the best asymptotically optimal solution obtained by the two-step optimization framework is outstanding, in both performance and complexity, by comparing with the local optimal solution.

First, we identify a set of asymptotically optimal solutions in the high SNR and user density region. Specifically, we consider the optimization of the asymptotic successful transmission probability $q_{K,\infty}(\mathbf{p})$, i.e., Problem 1 with $q_{K,\infty}(\mathbf{p})$ in (24) being the objective function, which has a much simpler form than $q_K(\mathbf{p})$ in (23).

Problem 3 (Asymptotic Optimization for $K > 1$):

$$\begin{aligned} \max_{\mathbf{p}} \quad & q_{K,\infty}(\mathbf{p}) \\ \text{s.t.} \quad & (1), (2). \end{aligned}$$

An optimal solution $\mathbf{p}^* \triangleq (p_i^*)_{i \in \mathcal{I}}$ to Problem 3 is an asymptotically optimal solution to Problem 1 for $K > 1$, and the resulting successful transmission probability $q_{K,\infty}^* \triangleq q_{K,\infty}(\mathbf{p}^*)$ is the asymptotically optimal successful transmission probability to Problem 1 for $K > 1$. In the following, we focus on solving Problem 3 to obtain an asymptotically optimal solution to Problem 1.

Note that $q_K(\mathbf{p})$ in (23) is a function of $\mathbf{T} \triangleq (T_n)_{n \in \mathcal{N}}$. Thus, we also write $q_{K,\infty}(\mathbf{p})$ as $q_{K,\infty}(\mathbf{T})$. We would like to further simplify Problem 3 by exploring the relationship between \mathbf{T} and \mathbf{p} . Now, we introduce a new optimization problem w.r.t. \mathbf{T} .

Problem 4 (Equivalent Asymptotic Optimization for $K > 1$):

$$\begin{aligned} \max_{\mathbf{T}} \quad & q_{K,\infty}(\mathbf{T}) \\ \text{s.t.} \quad & 0 \leq T_n \leq 1, \quad n \in \mathcal{N}, \end{aligned} \tag{26}$$

$$\sum_{n \in \mathcal{N}} T_n = K. \tag{27}$$

The optimal solution to Problem 4 is denoted as $\mathbf{T}^* \triangleq (T_n^*)_{n \in \mathcal{N}}$, and the optimal value of Problem 4 is given by $q_{K,\infty}(\mathbf{T}^*)$. The following lemma shows that Problem 3 and Problem 4 are equivalent.

Lemma 2 (Equivalence between Problem 3 and Problem 4): For any feasible solution \mathbf{T} to Problem 4, there exists \mathbf{p} satisfying (3) which is a feasible solution to Problem 3. For any feasible solution \mathbf{p} to Problem 3, \mathbf{T} satisfying (3) is a feasible solution to Problem 4. Furthermore, the optimal values of Problem 3 and Problem 4 are the same, i.e., $q_{K,\infty}(\mathbf{p}^*) = q_{K,\infty}(\mathbf{T}^*) = q_{K,\infty}^*$.

Proof: Please refer to Appendix F. ■

Based on Lemma 2, we first focus on solving Problem 4 for \mathbf{T}^* . It can be easily seen that Problem 4 is convex and Slater's condition is satisfied, implying strong duality holds. Using KKT conditions, we can solve Problem 4.

Theorem 4 (Optimization of \mathbf{T}): The optimal solution $\mathbf{T}^* = (T_n^*)_{n \in \mathcal{N}}$ to Problem 4 is given by

$$T_n^* = \min \left\{ \left[\frac{1}{c_{1,K}} \sqrt{\frac{a_n c_{2,K}}{\nu^*}} - \frac{c_{2,K}}{c_{1,K}} \right]^+, 1 \right\}, \quad n \in \mathcal{N}, \quad (28)$$

where ν^* satisfies

$$\sum_{n \in \mathcal{N}} \min \left\{ \left[\frac{1}{c_{1,K}} \sqrt{\frac{a_n c_{2,K}}{\nu^*}} - \frac{c_{2,K}}{c_{1,K}} \right]^+, 1 \right\} = K. \quad (29)$$

Here, $c_{1,K}$ and $c_{2,K}$ are given by (12) and (13), respectively.

Proof: Theorem 4 can be proved in a similar way to Theorem 2. We omit the details due to page limitation. ■

Remark 2 (Interpretation of Theorem 4): As illustrated in Fig. 3 (b), the structure of the optimal solution \mathbf{T}^* given by Theorem 4 is similar to the reverse water-filling structure. The file popularity distribution \mathbf{a} and the physical layer parameters (captured in $c_{1,K}$ and $c_{2,K}$) jointly affect ν^* . Given ν^* , the physical layer parameters (captured in $c_{1,K}$ and $c_{2,K}$) affect the caching probabilities of all the files in the same way, while the popularity of file n (i.e., a_n) only affects the caching probability of file n (i.e., T_n^*). These features for \mathbf{T}^* are similar to those for \mathbf{p}^* given by Theorem 2. Similar to Theorem 2, from Theorem 4, we know that files of higher popularity get more storage resources, and some files of lower popularity may not be stored. In addition, for a popularity distribution with a heavy tail, more different files can be stored. The optimal structure is similar to the reverse water-filling structure.

From Theorem 4, we have the following corollary.

Corollary 5 (Asymptotically Optimal Solution for $K > 1$): If $\frac{\sqrt{a_1}}{\sum_{n \in \mathcal{N}} \sqrt{a_n}} \leq \frac{c_{1,K} + c_{2,K}}{c_{1,K}K + c_{2,K}N}$ and $\frac{\sqrt{a_n}}{\sum_{n \in \mathcal{N}} \sqrt{a_n}} > \frac{c_{2,K}}{c_{1,K}K + c_{2,K}N}$, then we have

$$T_n^* = \left(K + \frac{c_{2,K}}{c_{1,K}} N \right) \frac{\sqrt{a_n}}{\sum_{n \in \mathcal{N}} \sqrt{a_n}} - \frac{c_{2,K}}{c_{1,K}} > 0, \quad n \in \mathcal{N}, \quad (30)$$

$$q_{K,\infty}^* = \frac{1}{c_{1,K}} \left(1 - \frac{(\sum_{n \in \mathcal{N}} \sqrt{a_n})^2}{N + K \frac{c_{1,K}}{c_{2,K}}} \right). \quad (31)$$

Here, $c_{1,K}$ and $c_{2,K}$ are given by (12) and (13), respectively.

Note that Corollary 5 can be interpreted in a similar way to Corollary 2. In addition, by Corollary 2 and Corollary 5, we can see that under certain conditions, $q_{K,\infty}^*$ increases with K . This indicates the tradeoff between the network performance and network storage resources.

Based on Lemma 2, we know that any \mathbf{p}^* in the convex polyhedron $\{\mathbf{p}^* : (32), (1), (2)\}$ is an optimal solution to Problem 3, i.e., an asymptotically optimal solution to Problem 1 for $K > 1$, where

$$\sum_{i \in \mathcal{I}_n} p_i^* = T_n^*, \quad n \in \mathcal{N}. \quad (32)$$

and \mathbf{T}^* is given by Theorem 4 or Corollary 5. In other words, we have a set of asymptotically optimal solutions in the high SNR and user density region.

Next, we obtain the best asymptotically optimal solution which achieves the optimal successful transmission probability in the general region among the set of asymptotically optimal solutions, i.e., $\{\mathbf{p}^* : (32), (1), (2)\}$. Specifically, substituting \mathbf{p}^* satisfying (32) into $q_K(\mathbf{p})$ in (23), we have

$$\begin{aligned} q_K(\mathbf{p}^*) &= \sum_{n \in \mathcal{N}} \frac{a_n}{T_n^*} \sum_{i \in \mathcal{I}_n} p_i^* \left(\sum_{k=1}^K \sum_{\mathcal{N}_i^1 \in \mathcal{SN}_i^1(k-1)} G_{n,i}(\mathcal{N}_i^1, \mathbf{T}_{i,-n}^*) f_k(T_n^*) \right) \\ &= \sum_{i \in \mathcal{I}} \left(\sum_{n \in \mathcal{N}_i} \frac{a_n}{T_n^*} \sum_{k=1}^K \sum_{\mathcal{N}_i^1 \in \mathcal{SN}_i^1(k-1)} G_{n,i}(\mathcal{N}_i^1, \mathbf{T}_{i,-n}^*) f_k(T_n^*) \right) p_i^* \triangleq q_K(\mathbf{p}^*, \mathbf{T}^*). \end{aligned}$$

For given \mathbf{T}^* , we would like to obtain the best asymptotically optimal solution which maximizes the successful transmission probability $q_K(\mathbf{p}^*, \mathbf{T}^*)$ in the general region among all the asymptotically optimal solutions in $\{\mathbf{p}^* : (32), (1), (2)\}$.

Problem 5 (Optimization of \mathbf{p}^ under given \mathbf{T}^* for $K > 1$):*

$$\begin{aligned} \overline{q_{K,\infty}^*} &\triangleq \max_{\mathbf{p}^*} q_K(\mathbf{p}^*, \mathbf{T}^*) \\ &s.t. \quad (32), (1), (2). \end{aligned}$$

Problem 5 is a linear programming problem. The optimal solution to Problem 5 can be obtained using the simplex method. To further reduce complexity, before applying the simplex method, we can first derive some caching probabilities which are zero based on the relationship between \mathbf{p}^* and \mathbf{T}^* in (32). In particular, for all $i \in \mathcal{I}_n$ and $n \in \{n \in \mathcal{N} : T_n^* = 0\}$, we have

Algorithm 3 Asymptotically Optimal Solution for $K > 1$

- 1: Obtain the optimal solution \mathbf{T}^* to Problem 4 based on Theorem 4 or Corollary 5.
 - 2: Determine \mathcal{I}' and choose $p_i^* = 0$ for all $i \in \mathcal{I}'$ according to (33).
 - 3: Obtain $\{p_i^* : i \in \mathcal{I} \setminus \mathcal{I}'\}$ by solving Problem 5 under the constraint in (33) using the simplex method.
-

$p_i^* = 0$; for all $i \notin \mathcal{I}_n$ and $n \in \{n \in \mathcal{N} : T_n^* = 1\}$, we have $p_i^* = 0$. Thus, we have

$$p_i^* = 0, \quad i \in \mathcal{I}', \quad (33)$$

where $\mathcal{I}' \triangleq \bigcup_{n \in \{n \in \mathcal{N} : T_n^* = 0\}} \mathcal{I}_n \cup (\mathcal{I} \setminus \bigcup_{n \in \{n \in \mathcal{N} : T_n^* = 1\}} \mathcal{I}_n)$. Then, we can compute the remaining caching probabilities for the communications in $\mathcal{I} \setminus \mathcal{I}'$ using the simplex method.

Therefore, by solving Problem 4 and Problem 5, we can obtain the best asymptotically optimal solution in the general region, using the method summarized in Algorithm 3.¹² Note that the computational complexity of Algorithm 3 is much smaller than that of Algorithm 2 due to the following reasons: (i) since \mathbf{T}^* from Theorem 4 (Corollary 5) is in closed-form, the complexity of Step 1 of Algorithm 3 is low; (ii) for most popularity distributions of interest, the cardinality of set $\{n \in \mathcal{N} : T_n^* > 0\}$ is much smaller than N , and hence, the number of combinations of possibly positive caching probability (i.e., $I - |\mathcal{I}'|$) is actually much smaller than the total number of combinations (i.e., I); and (iii) Step 3 of Algorithm 3 is of manageable complexity.

Now, we compare the proposed local optimal design \mathbf{p}^\dagger (Local Opt. obtained using Algorithm 2) and the best asymptotically optimal design \mathbf{p}^* (Asymp. Opt. obtained using Algorithm 3) using a numerical example. From Fig. 5, we can see that the performance of Asymp. Opt. is very close to that of Local Opt., even at moderate transmit SNR and user density. On the other hand, the average matlab computation time for \mathbf{p}^\dagger is 112 times of that for \mathbf{p}^* , indicating that the complexity of Local Opt. is much higher than that of Asymp. Opt. These demonstrate the applicability and effectiveness of the proposed Asymp. Opt. in the general transmit SNR and user density region.

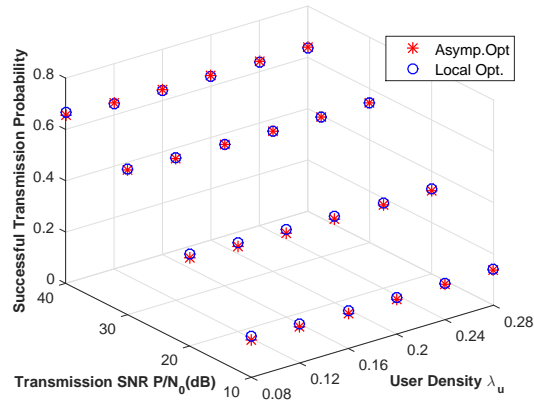


Fig. 5. Comparison between Local Opt. and Asymp. Opt. $N = 8$, $K = 4$, $\alpha = 4$, $\lambda_b = 0.01$, $W = 10 \times 10^6$, $\tau = 5 \times 10^5$, and $a_n = \frac{n^{-\gamma}}{\sum_{n \in \mathcal{N}} n^{-\gamma}}$ with $\gamma = 0.8$.

VI. NUMERICAL RESULTS

In this section, we compare the proposed asymptotically optimal design \mathbf{p}^* with three schemes.¹³ Baseline 1 refers to the design in which the most K popular files are stored at each BS, i.e., $T_n = 1$ for all $n = 1, \dots, K$ and $T_n = 0$ for all $n = K + 1, \dots, N$ [8], [9]. Baseline 2 refers to the design in which each BS selects K files in an i.i.d. manner with file n being selected with probability a_n [13]. Note that in Baseline 2, each BS may cache multiple copies of one file, leading to storage waste. Baseline 3 refers to the design in which each BS randomly selects one combination to cache according to the uniform distribution [4], i.e., $p_i = \frac{1}{I}$ for all $i \in \mathcal{I}$. Note that the three baseline schemes also adopt the multicasting scheme as in our design. In the simulation, we assume the popularity follows Zipf distribution, i.e., $a_n = \frac{n^{-\gamma}}{\sum_{n \in \mathcal{N}} n^{-\gamma}}$, where γ is the Zipf exponent. Note that a small γ means a heavy-tail popularity distribution.

Fig. 6 illustrates the successful transmission probability versus different parameters. From Fig. 6, we can observe that the proposed design outperforms all the three baseline schemes. In addition, the proposed design, Baseline 1 and Baseline 2 have much better performance than Baseline 3, as they exploit file popularity to improve the performance. The performance gap

¹²Note that Algorithm 3 is different from the method demonstrated in Fig. 1 of [9].

¹³When $N = 1000$, the complexity of Local Opt. is not acceptable. Thus, in Fig. 6, we only consider the proposed Asymp. Opt. and the three baseline schemes.

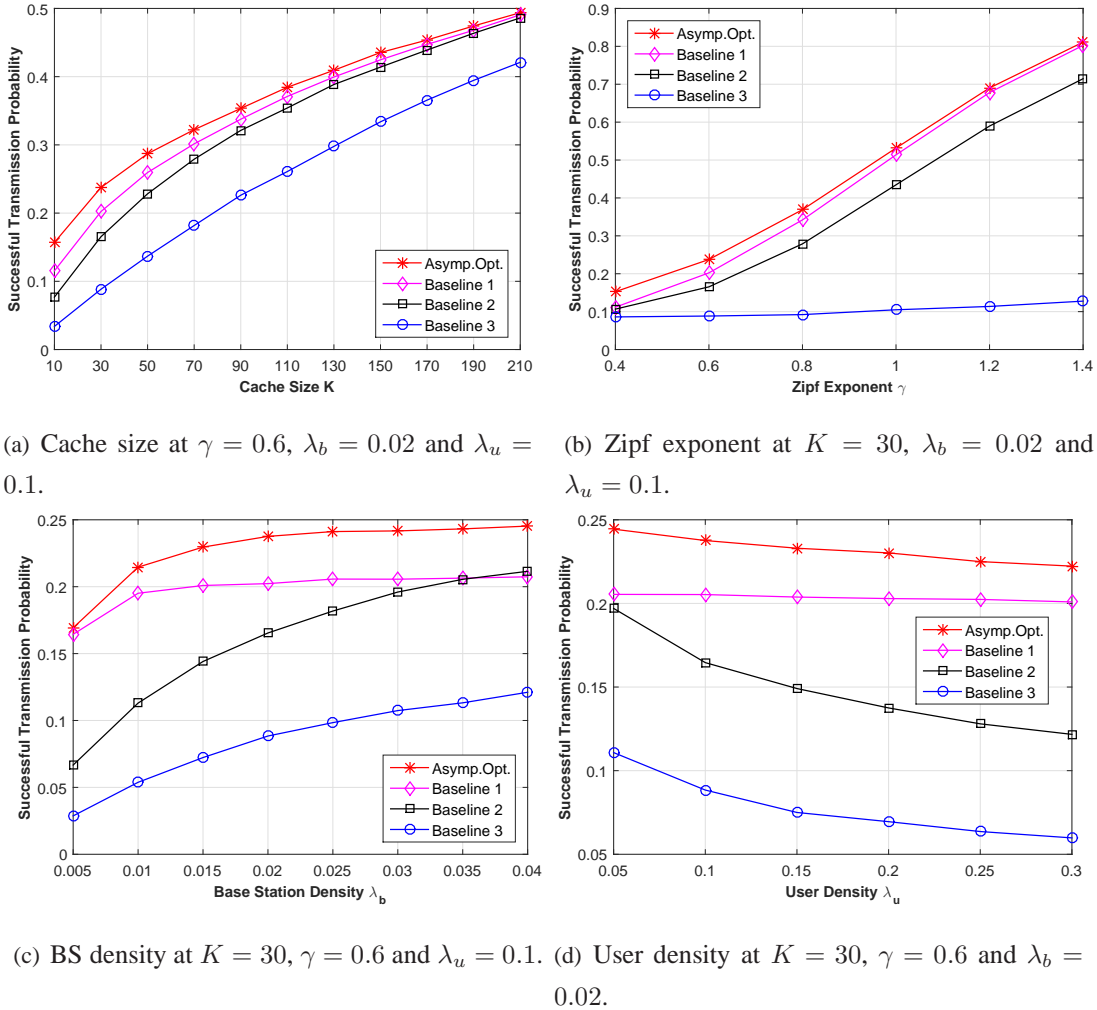


Fig. 6. Successful transmission probability versus cache size K , Zipf exponent γ , base station density λ_b and user density λ_u for $\frac{P}{N_0} = 30dB$, $\alpha = 4$, $W = 10 \times 10^6$, $\tau = 10^5$ and $N = 1000$.

between the proposed design and Baseline 1 is relatively large at small cache size K , small Zipf exponent γ , large BS density λ_b and small user density λ_u . This demonstrates the benefit of file diversity in these regions. Please note that the successful transmission probability in Fig. 6 is small due to the low file availability when K/N is small. This performance is achieved without backhaul cost or extra delay cost. Our goal here is to study how cache itself can affect the system performance.

Specifically, Fig. 6 (a) illustrates the successful transmission probability versus the cache size K . We can see that the performance of all the schemes increases with K . This is because as K increases, each BS can cache more files, and the probability that a randomly requested

file is cached at a nearby BS increases. Fig. 6 (b) illustrates the successful transmission probability versus the Zipf exponent γ . We can observe that the performance of the proposed design, Baseline 1 and Baseline 2 increases with the Zipf exponent γ much faster than Baseline 3. This is because when γ increases, the tail of popularity distribution becomes small, and hence, the average network file load decreases. The performance increase of Baseline 3 with γ only comes from the decrease of the average network file load. While, under the proposed design, Baseline 1 and Baseline 2, the probability that a randomly requested file is cached at a nearby BS increases with γ . Thus, the performance increases of the proposed design, Baseline 1 and Baseline 2 with γ are due to the decrease of the average network file load and the increase of the chance of a requested file being cached at a nearby BS. Fig. 6 (c) illustrates the successful transmission probability versus the BS density λ_b . We can see that the performance of all the schemes increases with λ_b . This is because the distance between a user whose requested file is cached in the network and its serving BS decreases, as λ_b increases. Fig. 6 (d) illustrates the successful transmission probability versus the user density λ_u . We can see that the performance of all the schemes decreases with λ_u . This is because the probability of a cached file being requested by at least one user increases, as λ_u increases. In addition, in Fig. 6 (c) The performance of the proposed design and Baseline 1 increases slower than that of Baseline 2 and Baseline 3; in Fig. 6 (d), the performance of the proposed design and Baseline 1 decreases slower than that of Baseline 2 and Baseline 3. The reason is that more different files are cached in the network under Baseline 2 and Baseline 3 than under the proposed design and Baseline 1. Note that under the proposed design, usually more than K but less than N different files are cached in the network; under Baseline 1, only K most popular files are cached in the network; under Baseline 2 and Baseline 3, all N files are cached in the network.

VII. CONCLUSION

In this paper, we consider the analysis and optimization of caching and multicasting in a large-scale cache-enabled wireless network. We propose a random caching and multicasting scheme with a design parameter. Utilizing tools from stochastic geometry, we first derive the successful transmission probability. Then, using optimization techniques, we develop an iterative numerical algorithm to obtain a local optimal design in the general region, and also derive a simple asymptotically optimal design in the high SNR and user density region.

Finally, we show that the asymptotically optimal design achieves promising performance in the general region with much lower complexity than the local optimal design.

APPENDIX A: PROOF OF THEOREM 1

First, as illustrated in Section IV-A, when $K = 1$, there are two types of interferers, i.e., the interfering BSs storing the file requested by u_0 and the interfering BSs storing the other files. Thus, we rewrite the SINR expression $\text{SINR}_{n,0}$ in (5) as

$$\text{SINR}_{n,0} = \frac{D_{0,0}^{-\alpha} |h_{0,0}|^2}{I_n + \sum_{m \in \mathcal{N}, m \neq n} I_m + \frac{N_0}{P}}, \quad (34)$$

where $\Phi_{b,n}$ ($n \in \mathcal{N}$) denotes the point process generated by BSs storing file n , $I_n \triangleq \sum_{\ell \in \Phi_{b,n} \setminus B_{n,0}} D_{\ell,0}^{-\alpha} |h_{\ell,0}|^2$, and $I_m \triangleq \sum_{\ell \in \Phi_{b,m}} D_{\ell,0}^{-\alpha} |h_{\ell,0}|^2$ ($m \in \mathcal{N}, m \neq n$). Due to the random caching policy and independent thinning [24, Page 230], we know that $\Phi_{b,m}$ is a homogeneous PPP with density $p_m \lambda_b$.

Next, we calculate the conditional successful transmission probability of file n requested by u_0 conditioned on $D_{0,0} = d$, denoted as $q_{1,n,D_{0,0}}(\mathbf{p}, d) \triangleq \Pr [W \log_2 (1 + \text{SINR}_{n,0}) \geq \tau | D_{0,0} = d]$. Based on (34), we have

$$\begin{aligned} & q_{1,n,D_{0,0}}(\mathbf{p}, d) \\ & \stackrel{(a)}{=} \mathbb{E}_{I_1, \dots, I_N} \left[\Pr \left[|h_{0,0}|^2 \geq (2^{\frac{\tau}{W}} - 1) D_{0,0}^\alpha \left(I_n + \sum_{m \in \mathcal{N}, m \neq n} I_m + \frac{N_0}{P} \right) \mid D_{0,0} = d \right] \right] \\ & \stackrel{(b)}{=} \mathbb{E}_{I_1, \dots, I_N} \left[\exp \left(- (2^{\frac{\tau}{W}} - 1) d^\alpha \left(I_n + \sum_{m \in \mathcal{N}, m \neq n} I_m + \frac{N_0}{P} \right) \right) \right] \\ & \stackrel{(c)}{=} \underbrace{\mathbb{E}_{I_n} \left[\exp \left(- (2^{\frac{\tau}{W}} - 1) d^\alpha I_n \right) \right]}_{\triangleq \mathcal{L}_{I_n}(s,d) \big|_{s=(2^{\frac{\tau}{W}}-1)d^\alpha}} \prod_{m \in \mathcal{N}, m \neq n} \underbrace{\mathbb{E}_{I_m} \left[\exp \left(- (2^{\frac{\tau}{W}} - 1) d^\alpha I_m \right) \right]}_{\triangleq \mathcal{L}_{I_m}(s,d) \big|_{s=(2^{\frac{\tau}{W}}-1)d^\alpha}} \\ & \quad \times \exp \left(- (2^{\frac{\tau}{W}} - 1) d^\alpha \frac{N_0}{P} \right), \end{aligned} \quad (35)$$

where (a) is obtained based on (34), (b) is obtained by noting that $|h_{0,0}|^2 \stackrel{d}{\sim} \exp(1)$, and (c) is due to the independence of the Rayleigh fading channels and the independence of the PPPs Φ_m ($m \in \mathcal{N}$). To calculate $q_{1,n,D_{0,0}}(\mathbf{p}, d)$ according to (35), we first calculate $\mathcal{L}_{I_n}(s, d)$ and

$\mathcal{L}_{I_m}(s, d)$ ($m \in \mathcal{N}, m \neq n$), respectively. The expression of $\mathcal{L}_{I_n}(s, d)$ is calculated below.

$$\begin{aligned} \mathcal{L}_{I_n}(s, d) &= \mathbb{E} \left[\exp \left(-s \sum_{\ell \in \Phi_{b,n} \setminus B_{n,0}} D_{\ell,0}^{-\alpha} |h_{\ell,0}|^2 \right) \right] = \mathbb{E} \left[\prod_{\ell \in \Phi_{b,n} \setminus B_{n,0}} \exp \left(-s D_{\ell,0}^{-\alpha} |h_{\ell,0}|^2 \right) \right] \\ &\stackrel{(d)}{=} \exp \left(-2\pi p_n \lambda_b \int_d^\infty \left(1 - \frac{1}{1 + sr^{-\alpha}} \right) r dr \right) \\ &\stackrel{(e)}{=} \exp \left(-\frac{2\pi}{\alpha} p_n \lambda_b s^{\frac{2}{\alpha}} B' \left(\frac{2}{\alpha}, 1 - \frac{2}{\alpha}, \frac{1}{1 + sd^{-\alpha}} \right) \right), \end{aligned} \quad (36)$$

where (d) is obtained by utilizing the probability generating functional of PPP [24, Page 235], and (e) is obtained by first replacing $s^{-\frac{1}{\alpha}} r$ with t , and then replacing $\frac{1}{1+t^{-\alpha}}$ with w .

Similarly, the expression of $\mathcal{L}_{I_m}(s, d)$ ($m \in \mathcal{N}, m \neq n$) is calculated as follows:

$$\begin{aligned} \mathcal{L}_{I_m}(s, d) &= \mathbb{E} \left[\exp \left(-s \sum_{\ell \in \Phi_{b,m}} D_{\ell,0}^{-\alpha} |h_{\ell,0}|^2 \right) \right] = \mathbb{E} \left[\prod_{\ell \in \Phi_{b,m}} \exp \left(-s D_{\ell,0}^{-\alpha} |h_{\ell,0}|^2 \right) \right] \\ &= \exp \left(-2\pi p_m \lambda_b \int_0^\infty \left(1 - \frac{1}{1 + sr^{-\alpha}} \right) r dr \right) \\ &= \exp \left(-\frac{2\pi}{\alpha} p_m \lambda_b s^{\frac{2}{\alpha}} B \left(\frac{2}{\alpha}, 1 - \frac{2}{\alpha} \right) \right). \end{aligned} \quad (37)$$

Substituting (36) and (37) into (35), we obtain $q_{1,n,D_{0,0}}(\mathbf{p}, d)$ as follows:

$$\begin{aligned} &q_{1,n,D_{0,0}}(\mathbf{p}, d) \\ &= \exp \left(-\frac{2\pi}{\alpha} p_n \lambda_b d^2 (2^{\frac{\tau}{\bar{w}}} - 1)^{\frac{2}{\alpha}} B' \left(\frac{2}{\alpha}, 1 - \frac{2}{\alpha}, 2^{-\frac{\tau}{\bar{w}}} \right) \right) \exp \left(- (2^{\frac{\tau}{\bar{w}}} - 1) d^\alpha \frac{N_0}{P} \right) \\ &\quad \times \exp \left(-\frac{2\pi}{\alpha} (1 - p_n) \lambda_b d^2 (2^{\frac{\tau}{\bar{w}}} - 1)^{\frac{2}{\alpha}} B \left(\frac{2}{\alpha}, 1 - \frac{2}{\alpha} \right) \right). \end{aligned} \quad (38)$$

Now, we calculate $q_{1,n}(\mathbf{p})$ by removing the condition of $q_{1,n,D_{0,0}}(\mathbf{p}, d)$ on $D_{0,0} = d$. Note that we have the p.d.f. of $D_{0,0}$ as $f_{D_{0,0}}(d) = 2\pi p_n \lambda_b d \exp(-\pi p_n \lambda_b d^2)$, as the BSs storing file n form a homogeneous PPP with density $p_n \lambda_b$. Thus, we have:

$$q_{1,n}(\mathbf{p}) = \int_0^\infty q_{1,n,D_{0,0}}(\mathbf{p}, d) f_{D_{0,0}}(d) dd = f_1(p_n),$$

where $f_1(p_n)$ is given by (10). Finally, by $q_1(\mathbf{p}) = \sum_{n \in \mathcal{N}} a_n q_{1,n}(\mathbf{p})$, we can prove Theorem 1.

APPENDIX B: PROOF OF COROLLARY 1

When $\frac{P}{N_0} \rightarrow \infty$, $\exp\left(-\left(2^{\frac{\tau}{W}} - 1\right) d^\alpha \frac{N_0}{P}\right) \rightarrow 1$. Thus, by (9), we have:

$$\begin{aligned} q_{1,\infty}(\mathbf{p}) &= 2\pi\lambda_b \sum_{n \in \mathcal{N}} a_n p_n \int_0^\infty d \exp\left(-\frac{2\pi}{\alpha} p_n \lambda_b \left(2^{\frac{\tau}{W}} - 1\right)^\frac{2}{\alpha} d^2 B' \left(\frac{2}{\alpha}, 1 - \frac{2}{\alpha}, 2^{-\frac{\tau}{W}}\right)\right) \\ &\quad \times \exp\left(-\pi\lambda_b p_n d^2\right) \exp\left(-\frac{2\pi}{\alpha} (1 - p_n) \lambda_b \left(2^{\frac{\tau}{W}} - 1\right)^\frac{2}{\alpha} d^2 B \left(\frac{2}{\alpha}, 1 - \frac{2}{\alpha}\right)\right) dd \\ &= 2\pi\lambda_b \sum_{n \in \mathcal{N}} a_n p_n \int_0^\infty d \exp\left(-\pi\lambda_b p_n \left(c_{2,1} + c_{2,1} \frac{1}{p_n}\right) d^2\right) dd \end{aligned}$$

Noting that $\int_0^\infty d \exp(-cd^2) dd = \frac{1}{2c}$ (c is a constant), we can solve the integral and prove Corollary 1.

APPENDIX C: PROOF OF THEOREM 2

The Lagrangian of Problem 2 is given by

$$L(\mathbf{p}, \boldsymbol{\eta}, \nu) = \sum_{n \in \mathcal{N}} \frac{a_n p_n}{c_{2,1} + c_{1,1} p_n} + \sum_{n \in \mathcal{N}} \eta_n p_n + \nu \left(1 - \sum_{n \in \mathcal{N}} p_n\right),$$

where $\eta_n \geq 0$ is the Lagrange multiplier associated with (1), ν is the Lagrange multiplier associated with (2), and $\boldsymbol{\eta} \triangleq (\eta_n)_{n \in \mathcal{N}}$. Thus, we have $\frac{\partial L}{\partial p_n}(\mathbf{p}, \boldsymbol{\eta}, \nu) = \frac{a_n c_{2,1}}{(c_{2,1} + c_{1,1} p_n)^2} + \eta_n - \nu$. Since strong duality holds, primal optimal \mathbf{p}^* and dual optimal $\boldsymbol{\eta}^*, \nu^*$ satisfy KKT conditions, i.e., (i) primal constraints: (1), (2), (ii) dual constraints $\eta_n \geq 0$ for all $n \in \mathcal{N}$, (iii) complementary slackness $\eta_n p_n = 0$ for all $n \in \mathcal{N}$, and (iv) $\frac{a_n c_{2,1}}{(c_{2,1} + c_{1,1} p_n)^2} + \eta_n - \nu = 0$ for all $n \in \mathcal{N}$. By (1), (ii), (iii) and (iv), we have: if $\nu < \frac{a_n}{c_{2,1}}$, then $\eta_n = 0$ and $p_n = \frac{1}{c_{1,1}} \sqrt{\frac{a_n c_{2,1}}{\nu} - \frac{c_{2,1}}{c_{1,1}}}$; if $\nu \geq \frac{a_n}{c_{2,1}}$, then $\eta_n = \nu - \frac{a_n c_{2,1}}{(c_{2,1} + c_{1,1} p_n)^2}$ and $p_n = 0$. Thus, we have $p_n^* = \left[\frac{1}{c_{1,1}} \sqrt{\frac{a_n c_{2,1}}{\nu^*} - \frac{c_{2,1}}{c_{1,1}}}\right]^+$. Combining (2), we can prove Theorem 2.

APPENDIX D: PROOF OF LEMMA 1

Let the random variable $Y_{m,n,i} \in \{0, 1\}$ denote whether file $m \in \mathcal{N}_{i,-n}$ is requested by the users associated with $B_{n,0}$ when $B_{n,0}$ contains combination $i \in \mathcal{I}_n$. When $B_{n,0}$ contains combination $i \in \mathcal{I}_n$, we have $K_{n,0} = 1 + \sum_{m \in \mathcal{N}_{i,-n}} Y_{m,n,i}$. Thus, we have

$$\begin{aligned} &\Pr[K_{n,0} = k | B_{n,0} \text{ contains combination } i \in \mathcal{I}_n] \\ &= \sum_{\mathcal{N}_i^1 \in \mathcal{S} \mathcal{N}_i^1(k-1)} \prod_{m \in \mathcal{N}_i^1} (1 - \Pr[Y_{m,n,i} = 0]) \prod_{m \in \mathcal{N}_{i,-n} \setminus \mathcal{N}_i^1} \Pr[Y_{m,n,i} = 0], \end{aligned} \quad (39)$$

where $k = 1, \dots, K$. The probability that $B_{n,0}$ contains combination $i \in \mathcal{I}_n$ is $\frac{p_i}{T_n}$. Thus, by the law of total probability, we have

$$\Pr[K_{n,0} = k] = \sum_{i \in \mathcal{I}_n} \frac{p_i}{T_n} \Pr[K_{n,0} = k | B_{n,0} \text{ contains combination } i \in \mathcal{I}_n],$$

where $k = 1, \dots, K$. Thus, to prove (21), it remains to calculate $\Pr[Y_{m,n,i} = 0]$. The p.m.f. of $Y_{m,n,i}$ depends on the p.d.f. of the size of the Voronoi cell of $B_{n,0}$ w.r.t. file $m \in \mathcal{N}_{i,-n}$ when $B_{n,0}$ contains combination $i \in \mathcal{I}_n$, which is unknown. We approximate this p.d.f. based on the p.d.f. of the size of the Voronoi cell to which a randomly chosen user belongs [23]. Under this approximation, we can calculate the p.m.f. of $Y_{m,n,i}$ using Lemma 3 of [23]: $\Pr[Y_{m,n,i} = 0] \approx \left(1 + 3.5^{-1} \frac{a_m \lambda_u}{T_m \lambda_b}\right)^{-4.5}$. Therefore, we complete the proof.

APPENDIX E: PROOF OF THEOREM 3

First, as illustrated in Section V-A, when $K > 1$, there are two types of interferers, i.e., the interfering BSs storing the combinations containing the file requested by u_0 and the interfering BSs without the desired file of u_0 . Thus, we rewrite the SINR expression $\text{SINR}_{n,0}$ in (5) as:

$$\text{SINR}_{n,0} = \frac{D_{0,0}^{-\alpha} |h_{0,0}|^2}{I_n + I_{-n} + \frac{N_0}{P}}, \quad (40)$$

where $\Phi_{b,n}$ is the point process generated by BSs containing file combination $i \in \mathcal{I}_n$ and $\Phi_{b,-n}$ is the point process generated by BSs containing file combination $i \in \mathcal{I}, i \notin \mathcal{I}_n$, $I_n \triangleq \sum_{\ell \in \Phi_{b,n} \setminus B_{n,0}} D_{\ell,0}^{-\alpha} |h_{\ell,0}|^2$, and $I_{-n} \triangleq \sum_{\ell \in \Phi_{b,-n}} D_{\ell,0}^{-\alpha} |h_{\ell,0}|^2$. Due to the random caching policy and independent thinning [24, Page 230], we obtain that $\Phi_{b,n}$ is an homogeneous PPP with density $\lambda_b T_n$ and $\Phi_{b,-n}$ is an homogeneous PPP with density $\lambda_b (1 - T_n)$.

Next, we calculate the conditional successful transmission probability of file n requested by u_0 conditioned on $D_{0,0} = d$ when the file load is k , denoted as

$$q_{k,n,D_{0,0}}(\mathbf{p}, d) \triangleq \Pr \left[\frac{W}{k} \log_2 (1 + \text{SINR}_{n,0}) \geq \tau | D_{0,0} = d \right].$$

Similar to (35) and based on (40), we have:

$$\begin{aligned} & q_{k,n,D_{0,0}}(\mathbf{p}, d) \\ &= \mathbb{E}_{I_n, I_{-n}} \left[\Pr \left[|h_{0,0}|^2 \geq \left(2^{\frac{k\tau}{W}} - 1\right) D_{0,0}^\alpha \left(I_n + I_{-n} + \frac{N_0}{P}\right) \mid D_{0,0} = d \right] \right] \\ &= \mathcal{L}_{I_n}(s, d) \Big|_{s=\left(2^{\frac{k\tau}{W}} - 1\right) d^\alpha} \mathcal{L}_{I_{-n}}(s, d) \Big|_{s=\left(2^{\frac{k\tau}{W}} - 1\right) d^\alpha} \exp \left(- \left(2^{\frac{k\tau}{W}} - 1\right) d^\alpha \frac{N_0}{P} \right). \quad (41) \end{aligned}$$

To calculate $q_{k,n,D_{0,0}}(\mathbf{p}, d)$ according to (41), we first calculate $\mathcal{L}_{I_n}(s, d)$ and $\mathcal{L}_{I_{-n}}(s, d)$, respectively. Similar to (36) and (37), we have

$$\mathcal{L}_{I_n}(s, d) = \exp\left(-\frac{2\pi}{\alpha} T_n \lambda_b s^{\frac{2}{\alpha}} B'\left(\frac{2}{\alpha}, 1 - \frac{2}{\alpha}, \frac{1}{1 + sd^{-\alpha}}\right)\right) \quad (42)$$

$$\mathcal{L}_{I_{-n}}(s, d) = \exp\left(-\frac{2\pi}{\alpha} (1 - T_n) \lambda_b s^{\frac{2}{\alpha}} B\left(\frac{2}{\alpha}, 1 - \frac{2}{\alpha}\right)\right). \quad (43)$$

Substituting (42) and (43) into (41), we obtain $q_{k,n,D_{0,0}}(\mathbf{p}, d)$ as follows:

$$\begin{aligned} & q_{k,n,D_{0,0}}(\mathbf{p}, d) \\ &= \exp\left(-\frac{2\pi}{\alpha} T_n \lambda_b d^2 \left(2^{\frac{k\tau}{W}} - 1\right)^{\frac{2}{\alpha}} B'\left(\frac{2}{\alpha}, 1 - \frac{2}{\alpha}, 2^{-\frac{k\tau}{W}}\right)\right) \exp\left(-\left(2^{\frac{k\tau}{W}} - 1\right) d^\alpha \frac{N_0}{P}\right) \\ & \times \exp\left(-\frac{2\pi}{\alpha} (1 - T_n) \lambda_b d^2 \left(2^{\frac{k\tau}{W}} - 1\right)^{\frac{2}{\alpha}} B\left(\frac{2}{\alpha}, 1 - \frac{2}{\alpha}\right)\right). \end{aligned} \quad (44)$$

Now, we calculate $q_{K,n}(\mathbf{p})$ by first removing the condition of $q_{k,n,D_{0,0}}(\mathbf{p}, d)$ on $D_{0,0} = d$. Note that we have the p.d.f. of $D_{0,0}$ as $f_{D_{0,0}}(d) = 2\pi T_n \lambda_b d \exp(-\pi T_n \lambda_b d^2)$, as the BSs storing file n form a homogeneous PPP with density $T_n \lambda_b$. Thus, we have:

$$\begin{aligned} & \int_0^\infty q_{k,n,D_{0,0}}(\mathbf{p}, d) f_{D_{0,0}}(d) dd \\ &= 2\pi T_n \lambda_b \int_0^\infty d \exp(-\pi T_n \lambda_b d^2) \exp\left(-\left(2^{\frac{k\tau}{W}} - 1\right) d^\alpha \frac{N_0}{P}\right) \\ & \times \exp\left(-\frac{2\pi}{\alpha} (1 - T_n) \lambda_b d^2 \left(2^{\frac{k\tau}{W}} - 1\right)^{\frac{2}{\alpha}} B\left(\frac{2}{\alpha}, 1 - \frac{2}{\alpha}\right)\right) \\ & \times \exp\left(-\frac{2\pi}{\alpha} T_n \lambda_b d^2 \left(2^{\frac{k\tau}{W}} - 1\right)^{\frac{2}{\alpha}} B'\left(\frac{2}{\alpha}, 1 - \frac{2}{\alpha}, 2^{-\frac{k\tau}{W}}\right)\right) dd. \end{aligned} \quad (45)$$

Finally, by $q_K(\mathbf{p}) = \sum_{n \in \mathcal{N}} a_n \sum_{k=1}^K \Pr[K_{n,0} = k] \int_0^\infty q_{k,n,D_{0,0}}(\mathbf{p}, d) f_{D_{0,0}}(d) dd$, we can prove Theorem 3.

APPENDIX G: PROOF OF LEMMA 2

Consider any feasible solution \mathbf{p} to Problem 3 satisfying (1) and (2). By (1) and (2), we know that \mathbf{T} satisfies (26). In addition, we have $\sum_{n \in \mathcal{N}} T_n = \sum_{n \in \mathcal{N}} \sum_{i \in \mathcal{I}_n} p_i = K \sum_{i \in \mathcal{I}} p_i = K$, i.e., \mathbf{T} satisfies (27). Thus, \mathbf{T} is a feasible solution to Problem 4. On the other hand, consider any feasible solution \mathbf{T} to Problem 4 satisfying (26) and (27). By the method in Fig. 1 of [9], we can easily construct a feasible solution \mathbf{p} to Problem 3. Therefore, we can show that Problem 3 is equivalent to Problem 4. In other words, the optimal values of the two problems are the same.

REFERENCES

- [1] Y. Cui, Y. Wu, and D. Jiang, "Analysis and optimization of caching and multicasting in cache-enabled information-centric networks," in *Global Communications Conference (GLOBECOM), 2015 IEEE*, Dec 2015.
- [2] X. Wang, M. Chen, T. Taleb, A. Ksentini, and V. Leung, "Cache in the air: exploiting content caching and delivery techniques for 5g systems," *Communications Magazine, IEEE*, vol. 52, no. 2, pp. 131–139, February 2014.
- [3] E. Bastug, M. Bennis, and M. Debbah, "Living on the edge: The role of proactive caching in 5g wireless networks," *Communications Magazine, IEEE*, vol. 52, no. 8, pp. 82–89, Aug 2014.
- [4] A. Liu and V. Lau, "Exploiting base station caching in MIMO cellular networks: Opportunistic cooperation for video streaming," *IEEE Trans. Signal Processing*, vol. 63, no. 1, pp. 57–69, Jan 2015.
- [5] S. Gitenis, G. S. Paschos, and L. Tassiulas, "Asymptotic laws for joint content replication and delivery in wireless networks," *Information Theory, IEEE Transactions on*, vol. 59, no. 5, pp. 2760–2776, May 2013.
- [6] K. Shanmugam, N. Golrezaei, A. Dimakis, A. Molisch, and G. Caire, "Femtocaching: Wireless content delivery through distributed caching helpers," *Information Theory, IEEE Transactions on*, vol. 59, no. 12, pp. 8402–8413, Dec 2013.
- [7] K. Poularakis, G. Iosifidis, and L. Tassiulas, "Approximation algorithms for mobile data caching in small cell networks," *Communications, IEEE Transactions on*, vol. 62, no. 10, pp. 3665–3677, Oct 2014.
- [8] E. Bastuđ, M. Bennis, M. Kountouris, and M. Debbah, "Cache-enabled small cell networks: Modeling and tradeoffs," *EURASIP Journal on Wireless Communications and Networking*, 2015.
- [9] B. Blaszczyszyn and A. Giovanidis, "Optimal geographic caching in cellular networks," in *IEEE Int. Conf. on Commun. (ICC)*, London, United Kingdom, June 2015, pp. 1–6.
- [10] D. Malak and M. Al-Shalash, "Optimal caching for device-to-device content distribution in 5g networks," in *Globecom Workshops (GC Wkshps), 2014*, Dec 2014, pp. 863–868.
- [11] S. Tamoor-ul-Hassan, M. Bennis, P. H. J. Nardelli, and M. Latva-aho, "Modeling and analysis of content caching in wireless small cell networks," *CoRR*, vol. abs/1507.00182, 2015. [Online]. Available: <http://arxiv.org/abs/1507.00182>
- [12] E. Altman, K. Avrachenkov, and J. Goseling, "Coding for caches in the plane." [Online]. Available: arXiv preprint arXiv:1309.0604
- [13] B. N. Bharath and K. G. Nagananda, "Caching with unknown popularity profiles in small cell networks," *CoRR*, vol. abs/1504.03632, 2015. [Online]. Available: <http://arxiv.org/abs/1504.03632>
- [14] D. Lecompte and F. Gabin, "Evolved multimedia broadcast/multicast service (eMBMS) in LTE-advanced: overview and Rel-11 enhancements," *IEEE Commun. Mag.*, vol. 50, no. 11, pp. 68–74, 2012.
- [15] K. Poularakis, G. Iosifidis, V. Sourlas, and L. Tassiulas, "Multicast-aware caching for small cell networks," in *IEEE WCNC*, April 2014, pp. 2300–2305.
- [16] N. Abedini and S. Shakkottai, "Content caching and scheduling in wireless networks with elastic and inelastic traffic," *IEEE/ACM Trans. Networking*, vol. 22, no. 3, pp. 864–874, June 2014.
- [17] B. Zhou, Y. Cui, and M. Tao, "Optimal dynamic multicast scheduling for cache-enabled content-centric wireless networks," in *Information Theory, 2015. ISIT 2015. IEEE International Symposium on*, June 2015.
- [18] D. Tse and P. Viswanath, *Fundamentals of Wireless Communication*. New York, NY, USA: Cambridge University Press, 2005.
- [19] J. Andrews, F. Baccelli, and R. Ganti, "A tractable approach to coverage and rate in cellular networks," *Communications, IEEE Transactions on*, vol. 59, no. 11, pp. 3122–3134, November 2011.
- [20] S. Singh, H. S. Dhillon, and J. G. Andrews, "Offloading in heterogeneous networks: modeling, analysis, and design insights," *IEEE Trans. Wireless Commun.*, vol. 12, no. 5, pp. 2484–2497, March 2013.

- [21] D. P. Bertsekas, *Nonlinear Programming*, 2nd ed. Belmont, MA: Athena Scientific, 1999.
- [22] S. Singh and J. Andrews, “Joint resource partitioning and offloading in heterogeneous cellular networks,” *Wireless Communications, IEEE Transactions on*, vol. 13, no. 2, pp. 888–901, Feb 2014.
- [23] S. M. Yu and S.-L. Kim, “Downlink capacity and base station density in cellular networks,” in *Modeling Optimization in Mobile, Ad Hoc Wireless Networks (WiOpt), 2013 11th International Symposium on*, May 2013, pp. 119–124.
- [24] M. Haenggi and R. K. Ganti, “Interference in large wireless networks,” *Foundations and Trends in Networking*, vol. 3, no. 2, pp. 127–248, 2009.